Research Paper

PAIN 166 (2025) 614–630

PAIN

EC C VIDEO

Epigenomic landscape of the human dorsal root ganglion: sex differences and transcriptional regulation of nociceptive genes

Úrzula Franco-Enzástiga[a], Nikhil N. Inturi[a], Keerthana Natarajan[a], Juliet M. Mwirigi[a], Khadijah Mazhar[a], Johannes C. M. Schlachetzki[b], Mark Schumacher[c], Theodore J. Price[a,*]

Abstract

Cell states are influenced by the regulation of gene expression orchestrated by transcription factors capable of binding to accessible DNA regions. To uncover if sex differences exist in chromatin accessibility in the human dorsal root ganglion (hDRG), where nociceptive neurons innervating the body are found, we performed bulk and spatial assays for transposase-accessible chromatin technology followed by sequencing (ATAC-seq) from organ donors without a history of chronic pain. Using bulk ATAC-seq, we detected abundant sex differences in the hDRG. In women, differentially accessible regions (DARs) mapped mostly to the X chromosome, whereas in men, they mapped to autosomal genes. Hormone-responsive transcription factor binding motifs such as EGR1/3 were abundant within DARs in women, while JUN, FOS, and other activating protein 1 factor motifs were enriched in men, suggesting a higher activation state of cells compared with women. These observations were consistent with spatial ATAC-seq data. Furthermore, we validated that *EGR1* expression is biased to female hDRG using RNAscope. In neurons, spatial ATAC-seq revealed higher chromatin accessibility in GABAergic, glutamatergic, and interferon-related genes in women and in Ca^{2+}-signaling-related genes in men. Strikingly, *XIST,* responsible for inactivating 1 X chromosome by compacting it and maintaining at the periphery of the nucleus, was found to be highly dispersed in female neuronal nuclei. This is likely related to the higher chromatin accessibility in X in female hDRG neurons observed using both ATAC-seq approaches. We have documented baseline epigenomic sex differences in the hDRG which provide important descriptive information to test future hypotheses.

Keywords: Epigenetics, Dorsal root ganglion, ATAC-seq, Sex differences, XIST, EGR1

1. Introduction

Women experience greater sensitivity to nociceptive pain compared with men[29] and lower tolerance to mechanical stimuli, as shown by epidemiological and experimental studies in healthy individuals.[4,18,39] Epidemiological evidence also indicates a higher prevalence and severity of neuropathic, inflammatory, and idiopathic pain in women compared with men,[18,52,58,81] and a greater number of clinical pain conditions,[6] which have been explained with sex dimorphic mechanisms of chronic pain,[50–52,67] using preclinical animal models in some cases.[24,30] Among the factors contributing to sex dimorphism in pain are hormonal, immunological, anatomical, and psychosocial factors.[60] There is an increasing interest in understanding the a priori differences between men and women to explain why women are more prone to chronic pain.[31,93]

Studies in humans demonstrate sex differences in gene expression for transcription factors and epigenetic remodelers in human dorsal root ganglion (hDRG) from thoracic vertebrectomy patients with chronic pain.[55,64] Moreover, in human tibial nerve and hDRG, as well as in the mouse DRG, there are sex differences in gene expression in individuals without any pain history suggesting underlying epigenetic differences at baseline that cause these divergent patterns of gene expression.[41,47,55,63,64,78,79] Decoding if sex differences in chromatin organization exist in hDRG before the onset of pathological pain can give insight into how and why these differences emerge.

Chromatin is a macromolecular complex found within the nuclear space composed of DNA, RNAs, and proteins. Epigenetic marks, like histone and DNA modifications, affect the degree of DNA compaction resulting in accessible regions termed euchromatin or compact regions called heterochromatin.[3] Chromatin accessibility is defined as the extent to which nuclear macromolecules can physically interact with DNA.[35] Besides its structural role, chromatin is also a dynamic entity that responds to cellular needs including transcription, DNA repair, and differentiation.[44,49] Dynamic changes in chromatin occur in the DRG in response to nerve injury and inflammation in animal models, demonstrating a functional role of epigenomic changes in chronic pain.[12,25,38,42,46,75,83,84] To date, very little is known

Sponsorships or competing interests that may be relevant to content are disclosed at the end of this article.

[a] *Center for Advanced Pain Studies, School of Behavioral and Brain Sciences, University of Texas at Dallas, Richardson, TX, United States,* [b] *Department of Cellular and Molecular Medicine, University of California, San Diego, La Jolla, CA, United States,* [c] *Department of Anesthesia and Perioperative Care and the UCSF Pain and Addiction Research Center, University of California, San Francisco, CA, United States*

**Corresponding author. Address: Center for Advanced Pain Studies, School of Behavioral and Brain Sciences, University of Texas at Dallas, 800 W Campbell Rd, BSB14.102, Richardson, TX 75080, United States. Tel.: +1 972-883-4311. E-mail address: theodore.price@utdallas.edu (T. J. Price).*

Supplemental digital content is available for this article. Direct URL citations appear in the printed text and are provided in the HTML and PDF versions of this article on the journal's Web site (www.painjournalonline.com).

http://dx.doi.org/10.1097/j.pain.0000000000003508

about the features of chromatin accessibility in hDRG. A previous study using microarray-based genomic and mRNA expression profiling found that expression quantitative trait loci help predict the contribution of genomic loci to pain phenotypes and are associated with open chromatin regions.[57] The identification of open chromatin is routinely measured with assays for transposase-accessible chromatin technology followed by sequencing (ATAC-seq).[8] A study of the human trigeminal ganglion (TG) found an association between single nucleus ATAC-seq (snATAC-seq) open chromatin and single nucleotide polymorphisms (SNPs) associated with migraine.[89]

We hypothesized that we would detect sex differences in the epigenomic landscape of the hDRG. We used bulk and spatial ATAC-seq coupled with bulk RNA sequencing (RNA-seq) to map the open chromatin accessibility landscape of female and male hDRG. We found pervasive differences in transcriptional regulatory programs between women and men that likely have important implications for understanding epidemiological and mechanism-based differences in nociceptive pain.

2. Materials and methods

2.1. Dorsal root ganglion tissue preparation

All human tissue procurement procedures were approved by the Institutional Review Board at the University of Texas at Dallas. Lumbar DRGs from human organ donors were obtained through a collaborative effort with the Southwest Transplant Alliance (STA). Donor medical and drug prescription history are provided by the STA, gathered through a questionnaire filled out by the donor's next of kin, or from available medical records. Right after dissection, human lumbar DRGs from male and female organ donors were either transported in artificial cerebral spinal fluid (aCSF) to be further processed within our facilities or frozen in dry ice right after dissection and stored in a −80°C freezer.

Dorsal root ganglion donor demographic information is provided in Table S1, http://links.lww.com/PAIN/C195. The inclusion criteria for this study considered adult donors aged 18 to 65 years who exhibited no signs of chronic pain or neuropathy and that did not have history of medications for chronic pain. The cutoff age of 65 years old was determined based on prior epigenomic studies, which indicated significant alterations in both men and women occurring notably after the age of 65.[45]

2.2. Bulk assay for transposase-accessible chromatin technology followed by sequencing on fresh human dorsal root ganglion

Immediately after dissection, human L4 or L5 DRGs from male and female organ donors (N = 5 women, N = 4 men) were transported in cold bubbled NMDG-aCSF pH 7.4 (93 mM NMDG, 2.5 mM KCl, 1.25 mM NaH_2PO_4, 30 mM $NaHCO_3$, 20 mM HEPES, 25 mM glucose, 5 mM ascorbic acid, 2 mM thiourea, 3 mM sodium pyruvate, 10 mM Mg_2SO_4, 0.5 mM $CaCl_2$, 12 mM N-acetylcysteine; osmolarity 310 mOsm)[85] in ice to our facilities. Using scissors, tissue was chopped in 2 mL of ice-cold nuclei isolation buffer.[48] This buffer contained: 250 mM sucrose, 25 mM KCl, 5 mM $MgCl_2$, 10 mM Tris-HCl pH 8.0, and 0.1% triton X-100. The total volume was transferred to a Dounce homogenizer. Overall, 5 strokes of the loose pestle and 15 strokes of the tight pestle were applied.[21] The homogenate was transferred to a conical tube and centrifuged at 100*g* for 8 minutes at 4°C. The supernatant was carefully removed without disrupting the soft pellet. Next, the pellet was resuspended in 2 mL of nuclei isolation buffer free of triton. After centrifugation at 100*g* for 8 minutes at 4°C, the supernatant was removed without disrupting the pellet. Subsequently, the nuclei were resuspended in 2 μm of nuclei isolation buffer without triton and filtered through a 40μm cell strainer. The number of isolated nuclei was counted using a hematocytometer. A total of 100,000 nuclei were aliquoted and centrifuged at 500*g* for 10 minutes at 4°C. The supernatant was then removed, and the pellet was utilized for the tagmentation reaction and DNA purification using the ATAC-seq kit from Active Motif kit, Carlsbad, CA (cat. no. 53150).

This Active Motif kit follows the general principles of ATAC-seq[8,9] and contains homodimers of the hyperactive Tn5 transposase bound to insert sequences containing polymerase chain reaction (PCR) handles (transposomes), which allow downstream amplification with sequencing adapters.[1] In brief, 50 μL of Tagmentation Master Mix (consisting of 2X tagmentation buffer, 10X phosphate-buffered saline (PBS), 0.5% digitonin, 10% tween 20, and assembled transposomes) was added to each sample. The tagmentation reaction was incubated at 37°C for 30 minutes in a thermomixer at 800 rpm. Subsequently, 250 μL of purification binding buffer and 5 μL of 3 M sodium acetate were added. DNA purification columns were employed to isolate the DNA and the tagmented DNA was eluted in 35 μL of DNA elution buffer. The amplification of tagmented DNA through PCR was carried out using i7- and i5-Illumina's Nextera-based adapters as per the provider's instructions. Pair-end 75-cycle sequencing reads were acquired on the Nextera500 sequencer or Nextera2000 sequencer. A total of 100 million reads were obtained from each hDRG.

2.3. RNA-seq on fresh human dorsal root ganglion

After isolating 100,000 nuclei from hDRG for bulk ATAC-seq, the remaining extracted nuclei were used to perform RNA extraction with the aim of sequencing and pairing bulk nucRNA-seq with ATAC-seq from the same sample. RNA was extracted from 4 male and 3 female hDRG samples, thus the pairing with ATAC-seq samples was performed in 7 out of 9 bulk ATAC-seq samples (Table S1, http://links.lww.com/PAIN/C195).

Total RNA from hDRG nuclei was purified using TRIzol. RNA peak profiles were analyzed using 5200 Fragment Analyzer and quantified with Qubit. RNA quality number was used to assess RNA Integrity (Table S2, http://links.lww.com/PAIN/C195). Illumina Tru-seq stranded RNA library prep was used to generate cDNA libraries according to the manufacturer's instructions. RNA sequencing was performed in a NextSeq 2000 sequencer. Single-end sequencing was performed in a multiplexed fashion by loading the samples on a P2 flow cell, averaging ~50 million reads per sample.

2.4. Spatial assays for transposase-accessible chromatin technology followed by sequencing on frozen human dorsal root ganglion

The frozen hDRGs were gradually embedded in Tissue-Tek optimal cutting temperature (OCT) compound in a cryomold by adding small volumes of OCT over dry ice to avoid thawing. A total of 8 hDRGs were used for these experiments (N = 3 women, N = 5 men) and demographic information of the organ donors is provided in Table S3, http://links.lww.com/PAIN/C195. All tissues were cryostat sectioned at 10 μm onto SuperFrost Plus charged slides (Thermo Fisher Scientific, Waltham, MA; Cat 12–550-15). Sections were only briefly thawed to adhere to the slide but were immediately returned to the −20°C cryostat chamber until completion of sectioning. The slides were removed from the cryostat and sent to AtlasXomics for further processing.[16,22] Spatial ATAC-seq (AXO-0303) consisted of the next steps: the tissue was fixed for 5 minutes with 0.2%

paraformaldehyde. Afterwards, the tissue was treated with glycine and left to dry. Then, a tissue permeabilization step was performed using 0.1% NP40 for 15 minutes. Tn5 transposition on the fixed hDRG sections was carried out for 30 minutes. Adapters containing a ligation linker were added to the preparation to be inserted in accessible genomic loci. Barcodes with linkers were introduced using microchannels and were ligated to the 5′ end of the Tn5 oligo through successive rounds of ligation. Human dorsal root ganglion sections were imaged to correlate spatially barcoded accessible chromatin with tissue morphology. A barcoded tissue mosaic was created, and reverse cross-linking was performed to release DNA fragments, which were then amplified through PCR for subsequent library preparation. Furthermore, 150 × 150 paired-end sequencing was performed using NextSeq 2000 with 15% PhiX. Sequencing depth was up to 300 million reads per hDRG section.

2.5. Processing of bulk assays for transposase-accessible chromatin technology followed by sequencing data

First, we verified the quality of raw sequencing fastq files using FastQC v0.11.7. We removed adapters using TrimGalore-0.6.6 and verified the quality of trimming using FastQC v0.11.7. Paired-end reads were mapped to the reference genome GRCh38/hg38 using Bowtie2. To remove unmapped reads, low-quality reads, or reads that mapped to mitochondrial DNA and PCR duplicates, we used Bamtools. Areas of open chromatin were identified by peak calling for each sample using Macs2 v.2.2.7.1 in keeping with Galaxy ATAC-seq data analysis.

Differential accessibility between male and female donors was analyzed using DiffBind, a package within the Bioconductor framework. During differential analysis, normalization was performed in a default mode. Next, we used HOMER annotatePeaks which uses the program assignGenomeAnnotation to efficiently assign ATAC-seq peaks to genomic annotations. The definitions of annotations were acquired in a default mode. Processing of transcription factor binding sites was performed using Transcription factor Occupancy prediction By Investigation of ATAC-seq Signal (TOBIAS[5]) in conjunction with human consensus transcription factor motifs from JASPAR. In brief, ATACorrect parameter was used to assess and correct the Tn5 transposase sequence preference of cutting sites. Putative transcription factor binding sites or transcription factor occupancy within peak regions were estimated using FootprintScore. Differential transcription factor binding sites in ATAC-seq reads between male and female hDRG were detected with BINDetect. Differentially accessible regions (DARs) were identified using DESeq2 v1.42.0.

2.6. Processing of RNA-seq data

We confirmed the quality of raw sequencing fastq files using FastQC v0.11.7. The STAR alignment tool (v2.7.10b) was employed for aligning sequenced reads to the human GENCODE reference genome (v38). Sequenced reads underwent trimming to reduce sequencing quality issues at both ends. Relative abundance quantified as transcripts per million (TPM) was generated using the Stringtie tool and HTseq for counts generation.

2.7. Processing of spatial assays for transposase-accessible chromatin technology followed by sequencing data

Processing of spatial ATAC-seq was performed by AtlasXomics, as previously reported.[16] Chromap was used to perform the alignment of sequenced reads to the human GENCODE reference genome (v38) and remove duplicates from fastq files.[92] Fragment files containing coordinates of sequenced DNA molecules mapping to barcodes were generated for downstream analysis. For data visualization, pixels on tissue samples were designated using AtlasXbrowser based on microscopy images to create Seurat-compatible metadata files. ArchR was used to process fragments files and the pixels not on tissue were removed. Data normalization and dimensionality reduction were applied to the data using ArchR's iterative latent semantic indexing, and subsequent graph clustering and uniform manifold approximation and projection (UMAP) embedding were performed. ArchR functions were used to acquire gene accessibility scores and matrices (gene score model), marker genes for clustering, and genome browser tracks. ShinyGO-080 was used to plot the chromosomal location of DAR-associated genes in the human genome.

2.8. In situ hybridization

Human dorsal root ganglia from nonpain donors were embedded in OCT using a cryomold over dry ice and sectioned. 10 μm sections for *XIST* and 20 μm sections for *EGR1* detection were placed onto SuperFrost Plus charged slides (Thermo Fisher Scientific, cat. no. 1255015). Two sections per hDRG separated by at least 100 μm from each other were obtained to capture 2 sets of neurons allowing for a diverse population to be analyzed. Sections were fixed in cold 10% formalin pH 7.4 for 15 minutes and then dehydrated sequentially in 50% ethanol for 5 minutes, 70% ethanol for 5 minutes, and 100% ethanol for 10 minutes at RT. The slides were allowed to dry briefly and hydrophobic boundaries around the tissue sections were drawn with ImmEdge PAP pen (Vector Laboratories, Newark, MA, cat. no. H-4000).

RNAScope Fluorescent Multiplex Reagent Kit (Advanced Cell Diagnostics [ACD], Newark, CA, cat. no. 323100) was used to detect target *EGR1* (ACD, cat. no. 457671), *XIST* (ACD, cat. no. 311231), and *SCN10A* (ACD, cat. no. 406291-C2) mRNAs in hDRGs. The sections were treated with hydrogen peroxide (ACD, cat. no. 322335) for 10 minutes at RT followed by a rinse with ddH_2O. Sections then underwent 5 seconds of protease III (ACD, cat. no. 322337) digestion followed by a quick wash in 1X PBS at RT. *EGR1* or *XIST* (channel 1) and *SCN10A* (channel 2) probes were mixed in a 50:1 ratio. The probe solution was added to the sections placed onto the HybEZ Slide Rack (ACD, cat. no. 310017), which was then placed inside the HybEZ tray (ACD, cat. no. 310012). Probes were hybridized at 40°C for 2 hours in HybEZ II Oven (ACD, cat. no. 321721). Sections were rinsed twice in 1X RNAScope Wash Buffer (ACD, cat. no. 310091) at RT for a couple of minutes each. The sections were stored in 5X SSC buffer (Sigma-Aldrich, Burlington, MA, cat. no. S6636) overnight at RT. The slides were rinsed twice with 1X wash buffer followed by amplification with Amp 1 for 30 minutes, Amp 2 for 30 minutes, and Amp 3 for 15 minutes at 40°C. Channel 1 probe was coupled with Cy3 for *EGR1* or *XIST* detection and channel 2 with Cy5 for *SCN10A* detection. After rinsing 2 times with 1X wash buffer, sections were incubated with 1:5000 DAPI in 1X PBS for 1 minute. Tissue sections underwent a rinse with 1X PBS before being air-dried completely and cover-slipped with ProLong Gold Antifade Mountant (Thermo Fisher Scientific, cat. no. P36930). Slides were imaged at 20X, 60X, and 100X magnification using the Olympus FV3000 RS confocal laser scanning microscope.

In situ hybridization analysis was performed using ImageJ Fiji version 2.14.0 by the Difference of Gaussians (DoG) edge detection method. For *EGR1* analysis, regions of interest (ROIs) were hand-drawn around each neuron avoiding lipofuscin on the

image hyperstack. Channels with target probe were separated from the hyperstack and duplicated. The 2 images underwent the application of Gaussian Blur with sigma values 1 and 2, respectively. The 2 resulting images with blurs were subtracted using the built-in Image Calculator feature in ImageJ Fiji which allowed for the detection of in situ hybridization puncta using the default threshold function. Thresholding values that allowed for as little noise as possible without compromising the signal were chosen for each channel. The Analyze Particles feature was used to analyze the number of puncta. The count readout was extracted from the images across the 10 donors which were then used to plot *EGR1* puncta count in *SCN10A* positive or negative neurons for each sex. *EGR1* puncta count data are presented as violin plots with thick line indicating the median and dotted lines indicating the quartiles.

Data were analyzed with Graphpad Prism V9 (Graphpad, San Diego, CA). Student t test was used to assess differences in puncta count between sexes. A $P < 0.05$ was considered statistically significant. Donor information for these experiments is provided in Table S4, http://links.lww.com/PAIN/C195. For *XIST* analysis, ROIs were hand-drawn around analyzed nuclei using DAPI as a guide. Dispersal of *XIST* was measured based on the dispersion of hybridization signal puncta in hand-draw ROIs that traced the analyzed nuclei. This area was divided by the total nuclear area stained with DAPI. Donor information for these experiments is provided in Table S5, http://links.lww.com/PAIN/C195.

3. Results

3.1. Global chromatin landscape in female and male human dorsal root ganglion

To characterize the epigenetic landscape of the hDRG, we performed ATAC-seq,[9] an unbiased approach to assess chromatin accessibility regions within the genome[70] on lumbar hDRG from 9 donors (N = 5 women, N = 4 men, **Fig. 1A**). This assay does not require prior knowledge of the epigenetic state of cells or the fine-tuning of transcription factors regulating gene expression.[27] Assay for transposase-accessible chromatin technology followed by sequencing leverages the efficient insertion of the cleavage enzyme Tn5 into DNA located in open chromatin regions. The molecular event of recognizing and cleaving DNA and adding Tn5 overhangs at the 5′ and 3′ ends of DNA is known as transposition (**Fig. 1B**). Donor information for all the samples that were used for bulk ATAC in hDRG is shown in Table S1, http://links.lww.com/PAIN/C195. After peak calling, we obtained a total of 669,749 peaks in female and 506,435 in male hDRG samples. At the global level, the distribution of called peaks in both female and male hDRG samples is concentrated near the transcription start site (TSS), with a notable accumulation of ATAC-seq signal directly at the TSS rather than in the immediate vicinity (**Fig. 1C**). The transcription start site enrichment (TSSe) score is an important quality control parameter in ATAC-seq that measures the ATAC-seq signal enrichment in the areas surrounding the reference set of TSSs in the genome. It is calculated as the sequencing depth for each 100 bp in the window within 1000 or 2000 bp on each side of the TSS normalized by the sequencing depth at the end flanks (100 bp at each end of the TSS). After computing the average score for each window around the TSS, the maximum value is considered as the TSSe score. As the TSSs are generally active regions in the DNA, they are expected to be enriched in accessible chromatin. We obtained a mean TSSe score of 3.17 (**Fig. 1D**), similar to other reports using postmortem human tissue.[13,32] Fraction of reads in peaks (FRiP), defined as the measure of how many of the total reads are located within the peaks, was greater than 0.13 on average. By mapping ATAC-seq peaks to genomic regions, we found that ~15% of peaks mapped within the putative promoter, ~40% were in distal intergenic regions, and ~35% were found in introns (**Fig. 1E**). The enrichment of accessible chromatin in intergenic regions suggests that distal regulatory sequences, such as enhancers and noncoding regulatory elements in *cis*, can be accessed to regulate gene expression. In many cases, peaks located mainly in promoters,[74] but also those harbored in the gene body (introns and exons) have been found to be good predictors of gene expression.[28] However, the proof of concept for the functionality of enhancers is tissue-specific and requires further experimentation.[80] As our results show that, at the global level, chromatin accessibility in hDRG showed similar annotation to called peaks between sexes, and the proportion was typical to other ATAC-seq reports,[88] we aimed to conduct a sex-specific analysis identifying specific genes to investigate whether sex differences in pain could be associated with chromatin structure.

3.2. Sex differences in chromatin accessibility in human dorsal root ganglion

By comparing ATAC-seq peaks in female and male samples, we found 3005 differentially accessible chromatin regions (DARs, false discovery rate (FDR) < 0.01, **Fig. 2A**; complete DAR list is supplied in Dataset S1, http://links.lww.com/PAIN/C195). Among these, 41 were identified as gene promoters in the female hDRG. Notably, most DARs were located on the X chromosome in genes such as *MAPD72*, *FRMPD4, PORCN, PNMA3,* and *TKTL1* (**Fig. 2A**). In men, 234 DARs were associated with gene promoters (±1 kb from TSS) on autosomal chromosomes and included genes such as *NR1D1*, *IRF2*, *CCNB1*, *DAPK3*, and *FOXO1* (**Fig. 2A**, promoter DAR list is supplied in Dataset S2, http://links.lww.com/PAIN/C195). The ATAC-seq principal component analysis (**Fig. 2B**) demonstrated that female and male samples clustered separately, consistent with the DAR analysis results. Representative sex-biased DARs around the TSS in female and male hDRG are shown in **Figures 2C and D**, respectively. X inactivation is known to balance X chromosome gene expression between sexes, although it is incomplete in some tissues and new regulatory functions associated with escape from X inactivation are still being discovered.[69] We observed a striking number of DARs in this chromosome in the female DRG likely consistent with a lack of X silencing in the hDRG in women or the presence of poised genes ready to be activated.

3.3. Enriched transcription factor binding sites in sex-biased differentially accessible regions in human dorsal root ganglion

In addition to chromatin accessibility, ATAC-seq data enables the prediction of transcription factor binding to open chromatin regions. With the aim of dissecting sex-specific transcriptional activity programs in hDRG, we analyzed the differential transcription factor binding motifs within accessible chromatin between sexes in hDRG using TOBIAS. For this analysis, differential binding scores with −log10 (*P*-value) larger than the 95th percentiles (top 5% in each direction) were considered significant.[5] In women, transcription factors of the early growth response (EGR) family such as EGR1 and EGR3, and members of the specificity protein (SP) family such as SP1, SP2, SP4, and SP9 footprints were more abundant compared with men. In men, we found a higher level of footprints for transcription factors that are part of the activating protein 1 (AP-1) family such as Jun Proto-Oncogene (JUN), Fos

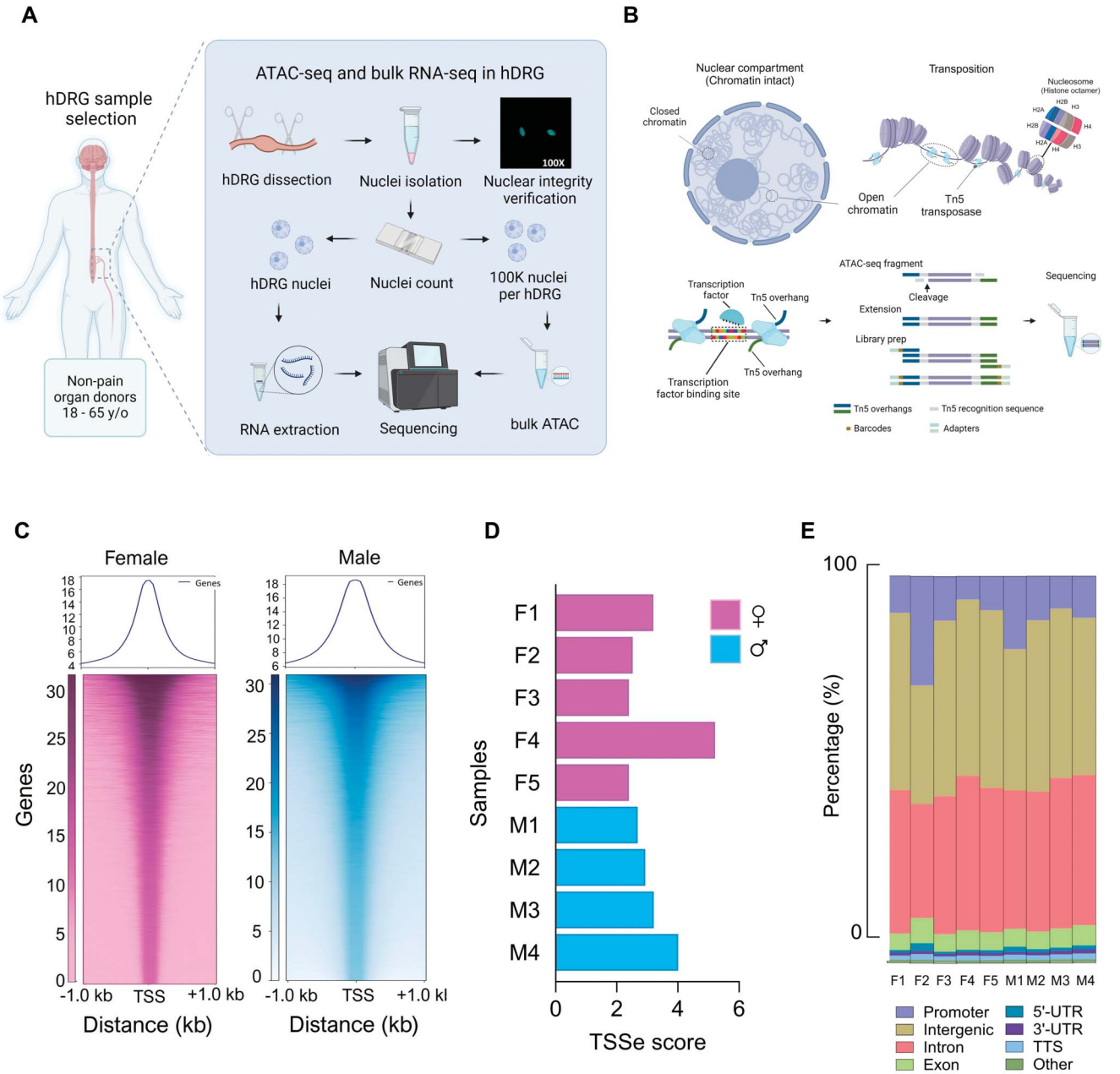

Figure 1. Uncovering the open chromatin landscape in hDRG. (A) Schematic of the study design for bulk ATAC-seq in fresh tissue. hDRG nuclei isolation and counting are performed. 100,000 nuclei per hDRG are used to perform ATAC-seq, while the leftover is used to extract RNA to perform paired analysis. (B) Overview of ATAC-seq transposition reaction and library preparation. During the transposition reaction, intact nuclei preserving the chromatin structure and DNA-bound proteins, such as histones and transcription factors, are treated with a mutant hyperactive Tn5 transposase. Acting as a homodimer, Tn5 enzymes cleave and simultaneously tag accessible DNA with Tn5 overhangs, which are insert sequences containing PCR handles. DNA is purified and PCR amplification proceeds. During the extension of PCR amplification, the Tn5 enzymatic cleavage left behind is filled in. Then, also during the PCR, the fragments are barcoded with Illumina adapters and amplified. ATAC-seq libraries are ready to be sequenced. (C) Heatmap shows chromatin accessibility around TSS ± 1 kb using aggregated peak enrichment scores from different female or male hDRG samples. Each row represents 1 consensus peak per gene spanning the TSS ordered by ATAC-seq signal intensity. ATAC-seq peaks are genomic regions enriched for Tn5 transposition events obtained after sequence analysis. Color represents the intensity of normalized chromatin accessibility. The metaplot on the top shows the mean ATAC-seq signal at the TSS. (D) TSSe score obtained for each sample as a quality control metric. (E) Proportion of ATAC-seq peaks associated with different genomic annotations in each hDRG sample. ATAC-seq, assays for transposase-accessible chromatin technology followed by sequencing; hDRG, human dorsal root ganglion; TTS, transcription termination site; TSS, transcription start site; TSSe, transcription start site enrichment; UTR, untranslated region.

Proto-Oncogene (FOS), FOS Like 2 (FOSL2), and Activating Trancription Factor 4 (ATF4). (**Figs. 3A and B**). The binding of transcription factors to the promoter of specific accessible genes was also an output of TOBIAS analysis. We found that the EGR1 transcription factor has binding sites in *ADORA2B*, a synaptic-localized GPCR gene; *CX3CL1*, a chemokine known to participate in paclitaxel-induced macrophage recruitment in the DRG[33]; and *JAK1*, a kinase essential for cytokine and growth factors signal transduction. EGR3 showed open chromatin binding sites in the promoter of *PIEZO2*, a mechanosensitive ion channel known for contributing to sensory neuron functions,[56] and *OXT, a* neuropeptide that suppresses action potential firing of DRG neurons.[26,62] Specificity protein 1 had binding sites on *TRPV2*, inflammation-related genes such as *TRAF1/4*, and heat shock proteins like

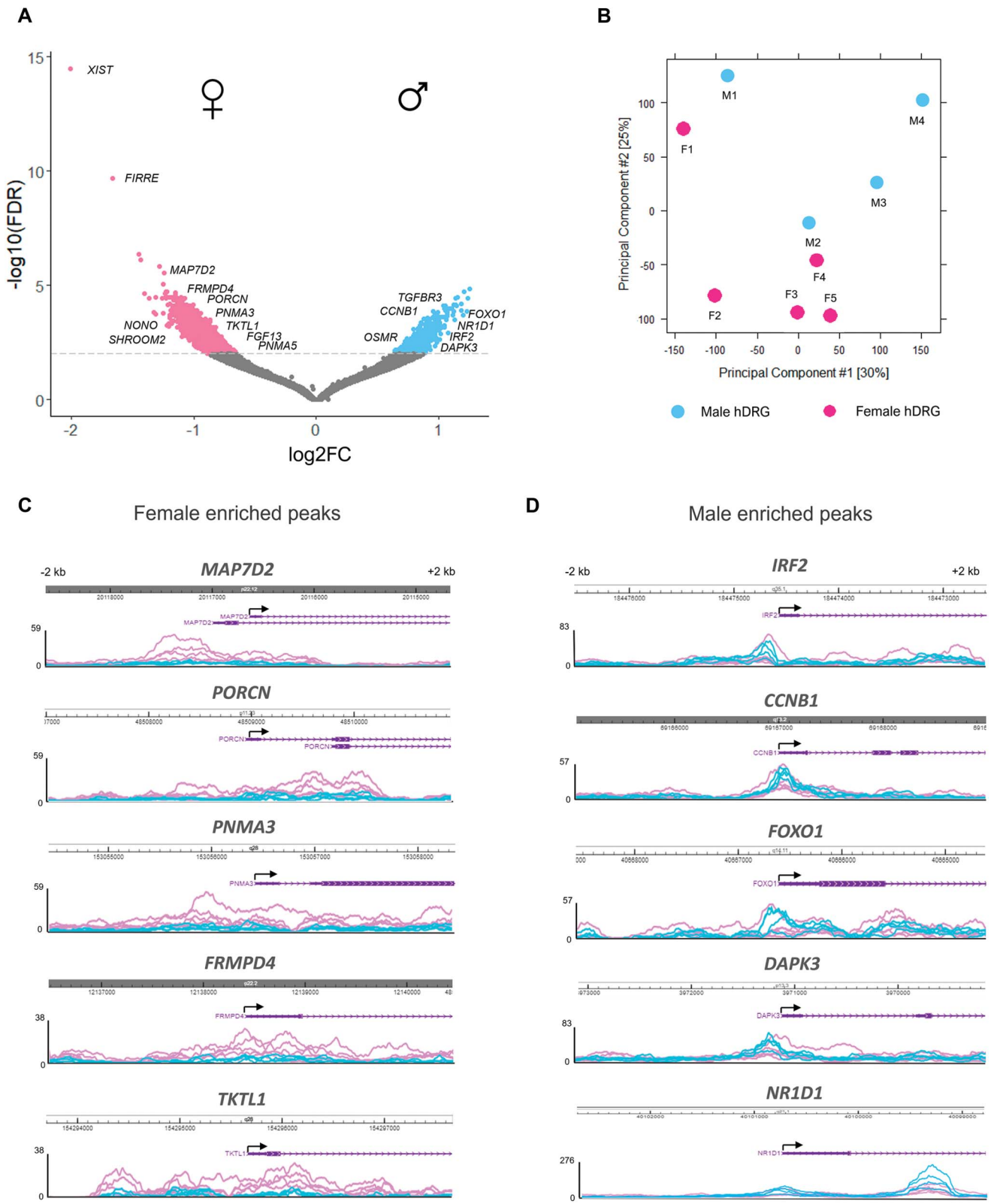

Figure 2. Analysis of sex differences in open chromatin regions in hDRG. (A) Volcano plot showing DARs in hDRG between sexes (N = 9, 5 female (pink), and 4 male (blue) postmortem hDRGs, FDR < 0.01) identified with DiffBind. (B) Principal component plot for ATAC-seq samples based on their similarity. (C) Genome browser views of ATAC-seq signal of DARs surrounding the transcription start site from female hDRG. (D) Representative genome browser tracks of DARs surrounding the transcription start site in male hDRG. DAR, differentially accessible region; ATAC-seq, assays for transposase-accessible chromatin technology followed by sequencing; FDR, false discovery rate; hDRG, human dorsal root ganglion.

HSF1. Finally, SP4 showed open chromatin binding sites in Ca^{2+}-signaling-related genes such as *CACNA1G* and *CARHSP1*, as well as the interferon regulatory transcription factor, *IRF6*. Examples of genes predicted to be regulated by the binding of EGR and/or SP transcription factors are depicted in **Figure 3C**. Activating protein 1 transcription factor and JDP2 binding sites in men had diverse

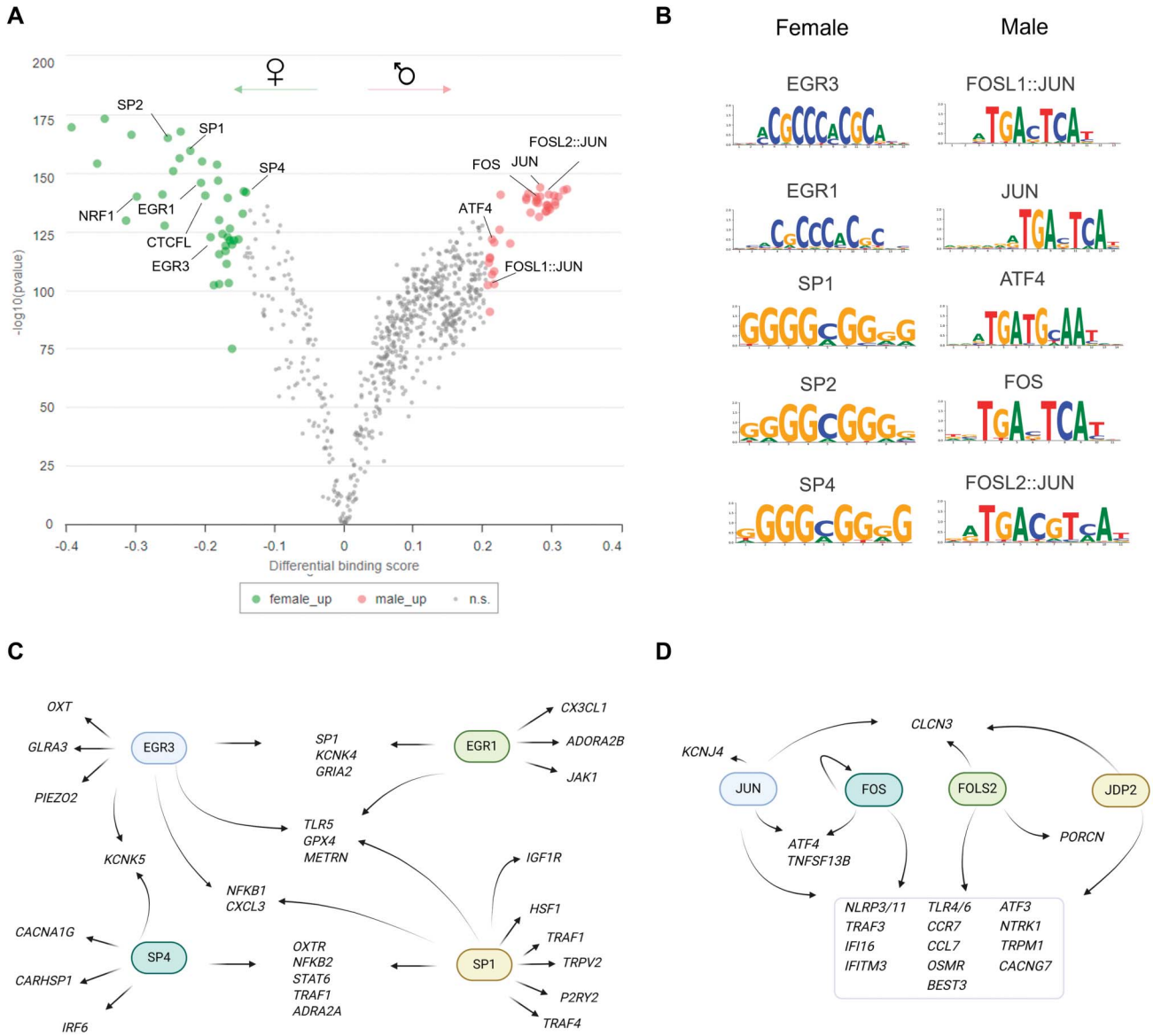

Figure 3. Sex differences in transcription factor binding motifs within ATAC-seq peaks. (A) Volcano plot showing the differential transcription factor footprints enriched in female and male hDRG identified with BINDetect (N = 9, 5 female and 4 male postmortem hDRGs, −log10 [*P*-value] > 95th percentiles). (B) Differential transcription factor consensus footprints in female and male hDRG defined by reference motif on JASPAR repository. (C) Genes predicted to bind EGR or SP factors due to transcription factor footprints in their promoters determined with TOBIAS. (D) Genes with transcription factor binding sites for AP-1 factors in their promoters identified with TOBIAS. AP-1, activating protein 1; ATAC-seq, assay for transposase-accessible chromatin technology followed by sequencing; EGR, early growth response; hDRG, human dorsal root ganglion; SP, specificity protein; TOBIAS, transcription factor occupancy prediction by investigation of ATAC-seq signal.

common targets in the accessible chromatin in hDRG, mainly in cytokine-related genes including *OSMR*, *IFI16*, *CCR7*, *NLRP3,* and *TLR4* (**Fig. 3D**). Together, these results suggest that women and men have different transcriptional activation programs. Whether these pathways play a role in sex differences in response to injury when additional transcription factors might be activated in these cells still needs to be investigated. However, it is a testable hypothesis that these baseline differences in molecular profiles could drive sex dimorphisms in pathological pain conditions.

3.4. Spatial assays for transposase-accessible chromatin technology followed by sequencing in human dorsal root ganglion

As we did not perform neuronal selection for our bulk ATAC-seq experiments in hDRG, and spatial information is lost during dissociation, we used spatial ATAC-seq to dissect the chromatin profile in neuronal barcodes in a similar fashion to how we have done previously in spatial RNA-seq.[79] Spatial ATAC-seq was performed in hDRG tissue sections from 8 donors (N = 5 men, N =3 women, Fig. S1, http://links.lww.com/PAIN/C196) using a microfluidic barcoding system, followed by next generation sequencing.[16]

We obtained 45,836 fragments on average in hDRG tissue, a TSSe score of 5.426, and a FRiP of 0.1276 of fragments of reads in peaks (Table S6, http://links.lww.com/PAIN/C195). The improved TSS score may be due to tissue preparation since DRGs for spatial experiments were immediately frozen in the operating room while DRGs for bulk ATAC-seq experiments were transported for 30 to 60 minutes in cold aCSF before nuclear isolation and subsequent tagmentation (see Methods). The average proportion of mitochondrial fragments was 4.15% (Table

S7, http://links.lww.com/PAIN/C195), and these reads were removed from the analysis. Assays for transposase-accessible chromatin technology followed by sequencing fragment size distribution showed a typical periodicity of ~200 bp corresponding to reads, consistent with the length of DNA protected by mono- or di-nucleosomes (200 or 400 bp), as well as nucleosome-free DNA (<100 bp) or open chromatin regions (Fig. S2, http://links.lww.com/PAIN/C196), all of which is consistent with typical nucleosome packing.[8]

In addition to neurons, there are at least 8 broadly defined cell types in hDRG.[7,34,54] This high hDRG cellular heterogeneity was also observed at the epigenomic level because unsupervised cell clustering in spatial ATAC-seq samples identified 9 groups of cells (**Fig. 4A**). Cluster 1 was classified as a neuronal cluster due to the abundance of chromatin accessibility in the *SNAP25* gene compared with other cell types. Furthermore, this cluster also shows chromatin activity for *CALCA* and *SCN10A* consistent with a neuronal phenotype (**Figs. 4B–D**). Cluster 2 showed enriched chromatin accessibility for the marker of satellite glial cells (SGCs), *FABP7* (**Fig. 4E**). The chromatin accessibility profile for cluster 3 had *CD300LB, IFI30*, *C5AR1*, *C1QB,* and *ABI3* among the top 30 most active genes, all of which are expressed by immune cells in the hDRG[7] (**Fig. 4F**). According to the hDRG harmonized atlas,[7] the top 30 most active genes for the cluster 5 exhibited enrichment for immune-related genes, such as *OLR1*, *MS4A7*, *TYROBP,* and *CORO1A*. Interestingly, this cluster also showed enrichment for macrophage markers such as *CD163, ARHGAP30, SIRPB2,* and *PLCB2*. Thus, we classified cluster 5 as immune macrophage enriched (**Fig. 4G**). Cluster 6 showed enriched chromatin accessibility in *SCN7A* likely representing the nonmyelinating Schwann cell cluster (**Fig. 4H**). Cluster 7 showed enriched chromatin accessibility in *PRX* and *MPZ* representing the myelinating Schwann cell cluster (**Fig. 4I**). A fibroblast cluster was identified by the gene activity of *DCN* and *FMOD* in cluster 8 (**Fig. 4J**). Cluster 9 was identified as the endothelial cluster due to abundant *CLDN5* gene accessibility (**Fig. 4K**). Cluster 4 was more challenging to classify. This cluster showed chromatin accessibility in genes such as *PODN* and *FOXD1*, which are expressed in fibroblasts in hDRG suggesting this cluster is composed of a subtype of fibroblast in the hDRG. Cell type composition in hDRG shows consistent cluster proportion between samples and sexes (**Fig. 4L**). The number of unique fragments per barcode exceeded the minimum values required to be considered high quality in all the clusters ($\log_{10}$ nFrag = 3, **Fig. 4M**). Transcription start site enrichment scores values per cluster and nucleosome ratio are depicted in Fig. S3, http://links.lww.com/PAIN/C196. The number of final peaks identified across all donors was 303,850, and the genomic annotation proportion was higher in intron and distal peaks, similar to our bulk ATAC-seq experiments (**Fig. 4N**).

3.5. Pseudo-bulk analysis of spatial assays for transposase-accessible chromatin technology followed by sequencing data

We conducted a pseudo-bulk differential analysis between sexes using the reads from all the clusters in spatial ATAC-seq to have a general overview of sex differences in hDRG chromatin accessibility, which we hypothesized would be similar to our bulk ATAC-seq data (**Fig. 5**). In **Figure 5A**, we show that the number of fragments per barcode and the distribution of reads in the UMAP were similar between female and male hDRG samples (**Fig. 5B**). Our analysis showed DARs in 3796 genes in female hDRG vs 3827 genes in men (**Fig. 5C**). In women, a significant proportion of DARs was located on the X chromosome consistent with our bulk ATAC-seq findings (**Fig. 5D**). These findings align with our bulk ATAC-seq results. Genes such as *NONO*, *MAPD7*, *FRMPD4*, *PORCN*, *FGF13,* and *TKTL1* shown in female bulk ATAC-seq were also found to be differentially accessible in female spatial ATAC-seq data. Spatial ATAC-seq also revealed female DARs in genes outside the X chromosome such as *ERBB4*, GABAergic genes including *GABRG1/2*, *GABRA5*, *GABRB3*, *GABRB1*, *GABRA2/4*, and other neuronal genes such as (Brain-derived neurotrophic factor) *BDNF*, *BDNF-AS*, *RELN*, *SCN9A*, *GRIA4,* and *GRIN2B* (Dataset S3, http://links.lww.com/PAIN/C195). It is important to mention that most of these genes are also significantly differentially accessible when only autosomes are analyzed, which validates our results (data not shown).

On the other hand, in men, the peaks spanned the whole genome, with a higher abundance of DARs in genes located on chromosomes 17 and 19 (**Fig. 5E**). Furthermore, a considerable amount of the genes with DARs in promoters in our bulk ATAC-seq data were also found to be biased towards men in the spatial ATAC-seq. We found male hDRG DAR-associated genes such as *FOS*, *FOSL2*, *NR1D1*, *IRF2,* and *FOXO1*. The male hDRG DAR list also included genes encoding for neurotrophic tyrosine kinase gene *NTRK1* and cation channels such as *TRPV2/4*. Interestingly, the male hDRG DAR list also comprised circadian-related genes such as *BHLHE40* and *CSNK1D,* cytokines such as *CSF1R*, *CCL2*, *IL4/6R*, and alarmins like *HMGA1*. Hormonal-associated genes such as *INSR* and *THRA* were also found to be epigenetically more active in men. Finally, genes encoding for epigenetic remodelers such as *DOT1L*, *HDAC4*, *JARID2,* and *ARID5B* were found in male hDRG.

Transcription factor (TF) motif enrichment analysis allowed us to infer differential binding sites in spatial ATAC-seq data. In women, transcription factors such as TEAD1/4, NR3C1, AR, and PGR were enriched in the spatial ATAC-seq dataset. In men, peaks in DARs again belonged to the AP-1 family, such as FOSB, or AP-1 interacting factor-like BACH1/2 (**Fig. 5F**).

3.6. Sex differences in chromatin accessibility in human dorsal root ganglion neurons determined with spatial assays for transposase-accessible chromatin technology followed by sequencing

A primary motivation of our spatial ATAC-seq approach was to identify potential sex differences in neurons in hDRG. To examine this, we compared chromatin accessibility in the neuronal-enriched cluster between sexes (**Fig. 6**). Differential analysis with DESeq2 analysis revealed DARs associated with 1665 genes in women and 1089 genes in men ($P_{adj} < 0.01$, **Fig. 6A**, Dataset S4, http://links.lww.com/PAIN/C195). Similar to what we observed previously with bulk ATAC-seq or the pseudo-bulk analysis of spatial ATAC-seq data, most of the peaks in women were located on the X chromosome ($P_{adj} < 0.01$, 643 out of 1665 genes, **Fig. 6B**). In male neurons, the genes were distributed across the entire genome, and again, there was a higher abundance observed on chromosomes 17 and 19 (**Fig. 6C**).

The analysis of gene ontology of genes associated with DARs between sexes showed that glutamatergic genes such as *GRIA2* and *GRIA4* to be found in the top 100 DARs in female hDRG chromatin. GABAergic genes such as *GABRB1*, *GABRE*, and *GABRA1/2/3/6* were also DARs in female hDRG within the differential female gene set. Enrichment analysis of accessible regions showed an association between open chromatin regions and glutamate receptor activity as the main gene ontology enriched molecular function category (P_{val}: 0.00001581, **Fig. 6D**) determined with EnrichR.[36] Interestingly, neurons in female

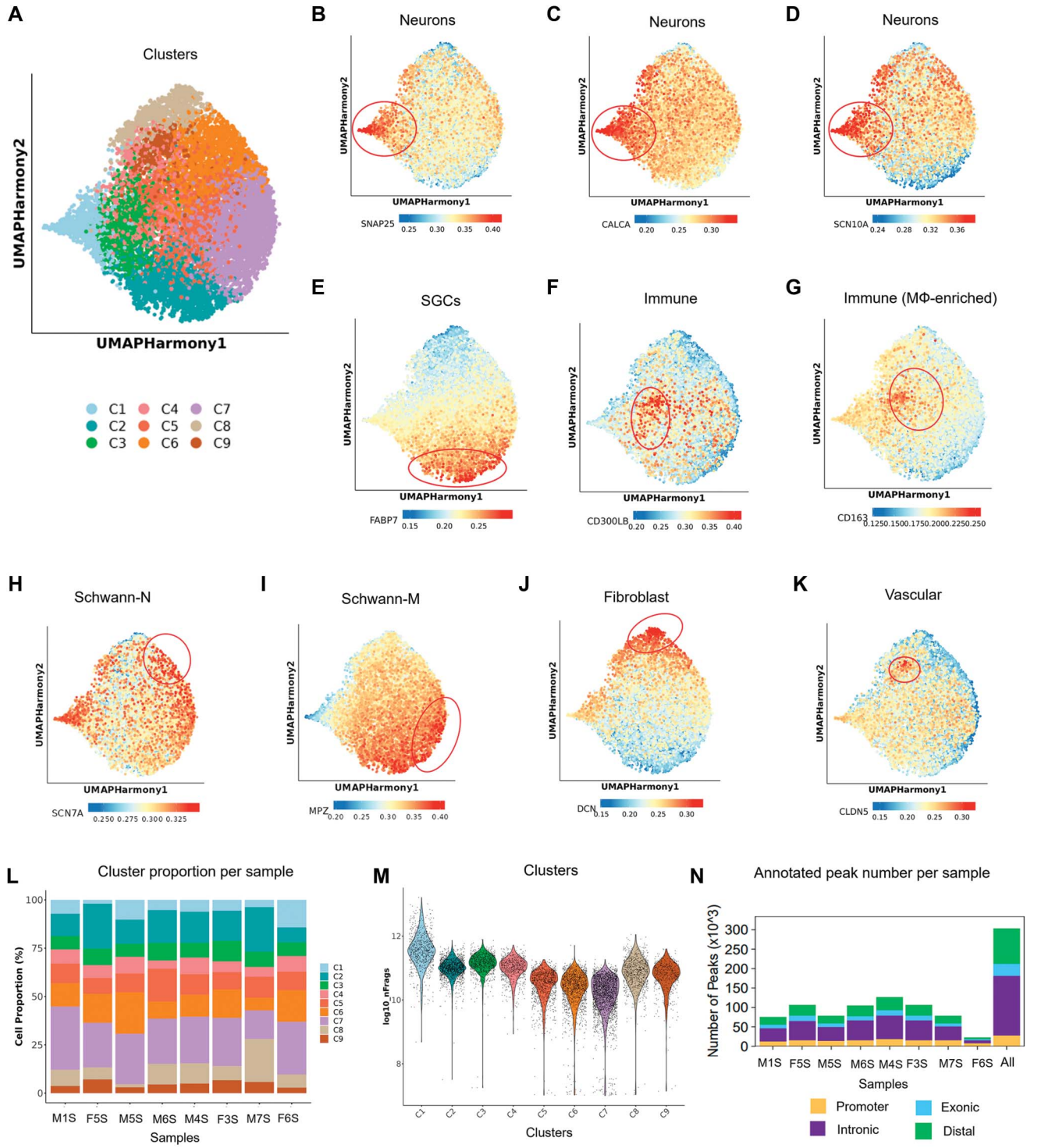

Figure 4. Characteristics of spatial ATAC-seq in hDRG. (A) UMAP plot showing the 9 clusters generated by Seurat workflow. (B–D) UMAP plots of the chromatin accessibility of gene markers that were used to label the neuronal cluster. (E–K) UMAP plot showing cellular populations other than neurons, including satellite glial cells (E), immune cells (F), immune cells enriched in macrophages (G), Schwann-N cells (H), Schwann-M cells (I), fibroblasts (J), and vascular cells (K). (L) Consistent cluster proportion in each sample. (M) Violin plot shows number of unique fragments per cluster. (N) Number of peaks identified across all donors (all), and within samples associated and their genomic annotations: promoter, intron, exon, and intergenic (N = 3 women, N =5 men; samples M5S, M6S, M7S, and F6S belonged to donors whose samples had not been used before for bulk ATAC-seq. Frozen hDRG samples from donors M1, M4, F3, and F5 were used for spatial ATAC-seq and are labeled as M1S, M4S, F3S, and F5S). ATAC-seq, assays for transposase-accessible chromatin technology followed by sequencing; hDRG, human dorsal root ganglion; UMAP, uniform manifold approximation and projection.

donors also showed DARs in *ACE2*, some interferon-related genes such as *IFNB1*, *IFNA8*, *IFIT3, TLR7,* and *CASP4*, and centromere genes such as *CENPE/W* compared with men.

In male neurons, genes such as *GRIK3* and *PTPRS* were found among DARs compared with women. Furthermore, voltage-gated Ca^{2+} channel-related genes such as *CACNA1G, CACNA1I,* and *CACNA2D2* were found in the male DAR gene set. Interestingly, *TRPV3* was also a DAR in men compared with female neurons. Gene ontology analysis of the male DAR gene set revealed a high abundance of calcium

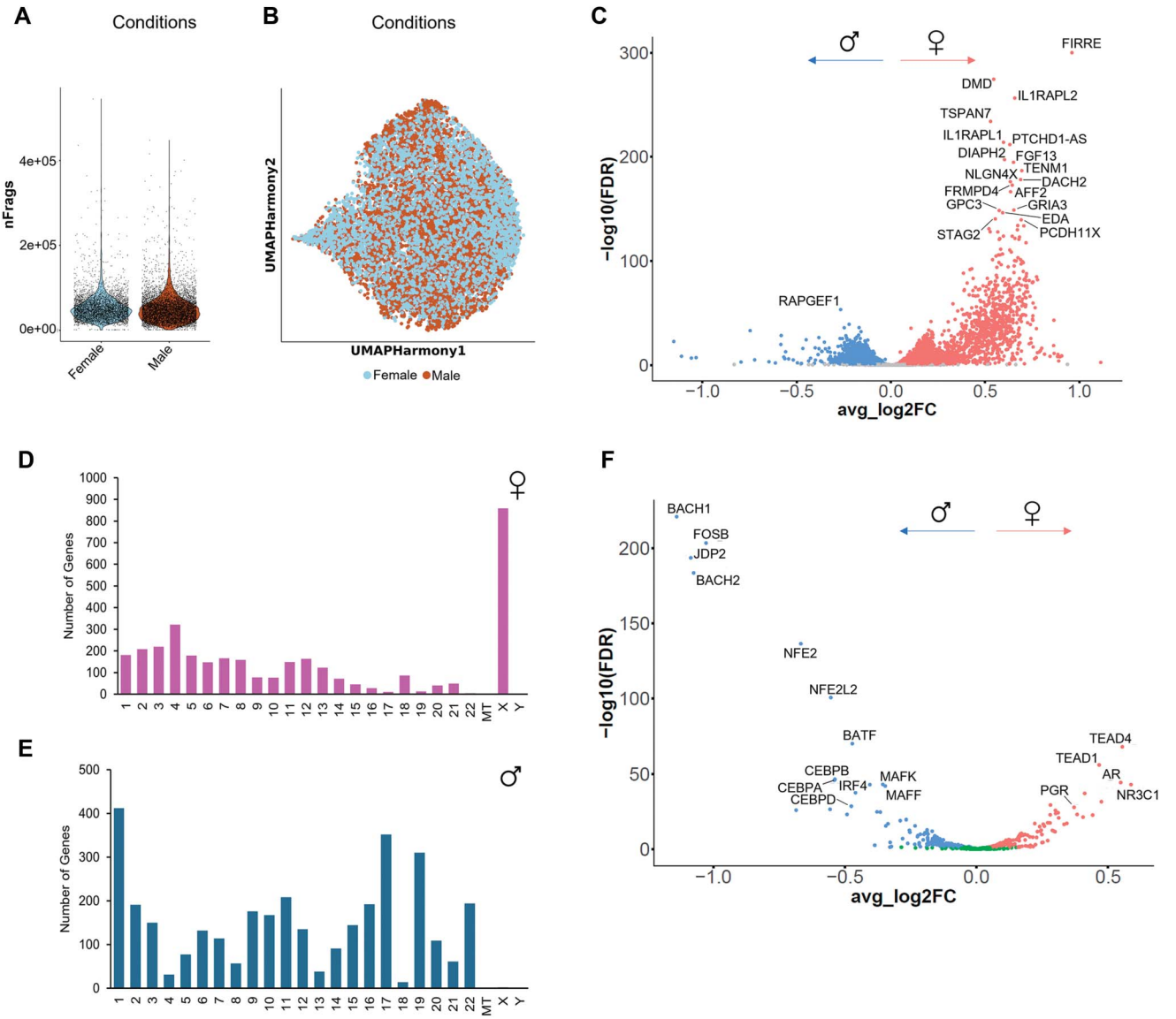

Figure 5. Differential spatial ATAC-seq signal in hDRG between sexes. Analysis of sex differences in chromatin gene activity in hDRG. (A) Number of fragments per barcode in female and male hDRG samples. (B) UMAP of female and male barcode distribution along hDRG cellular populations. (C) Volcano plot showing differential ATAC-seq gene activity in a pseudo-bulk fashion in hDRG in women vs men (N = 4 female, 5 male postmortem hDRGs), $P_{adj} < 0.01$ identified with ArchR. (D) Genome location of DARs in female spatial ATAC-seq spanning the human chromosomes generated with ShinyGO. (E) Genomic position of DARs in male hDRG. (F) Volcano plot showing differential transcription factor binding sites in female vs male hDRG (N = 3 female, 5 male postmortem hDRGs), $P_{adj} < 0.1$ identified with ArchR. ATAC-seq, assays for transposase-accessible chromatin technology followed by sequencing; DAR, differentially accessible region; hDRG, human dorsal root ganglion; UMAP, uniform manifold approximation and projection.

channel activity in the molecular function category (P_{val} = 0.00165, **Fig. 6E**).

Finally, we analyzed the neuronal cluster for enrichment of transcription factor binding sites in the DARs between women and men. In women, *EGR1*, *TEAD1/3/4*, *NR3C1, AR,* and *PGR* were enriched, and factors of the AP-1 family including *JUN* and *FOSB* as well as *IRF4* were found enriched in men (**Fig. 6F**).

3.7. EGR1 expression in human dorsal root ganglion

One of the outcomes that showed consistency in bulk and spatial ATAC-seq was the bias toward women in the footprint scores for the transcription factor EGR1 in hDRG, and specifically in neurons. With the aim of validating this consistent finding, we sought to assess the expression of *EGR1* in hDRG using in situ hybridization. We found that *EGR1* is expressed in female and male hDRG *SCN10A* (+) and (−) neurons, but also in cells surrounding neurons, likely satellite glial or immune cells (**Figs. 7A and B**). We quantified the number of *EGR1* mRNAs localized to hDRG neurons and found it to be more abundant in women compared with men (**Fig. 7C**). This sexual dimorphism was statistically significant in *SCN10A* (+), but not *SCN10A* (−) cells in women (**Figs. 7D and E**). Our analysis also showed that women have a higher number of *EGR1* (+) *SCN10A* (+) cells compared with men (57.9% vs 29.71%, respectively, **Fig. 7F**). These results are consistent with our datasets. The combined identification of *EGR1* female-biased expression and the prominent abundance of regulatory binding sites in female hDRG renders the transcriptional activity of *EGR1* a strong candidate for a female-biased regulator of gene expression in hDRG neurons.

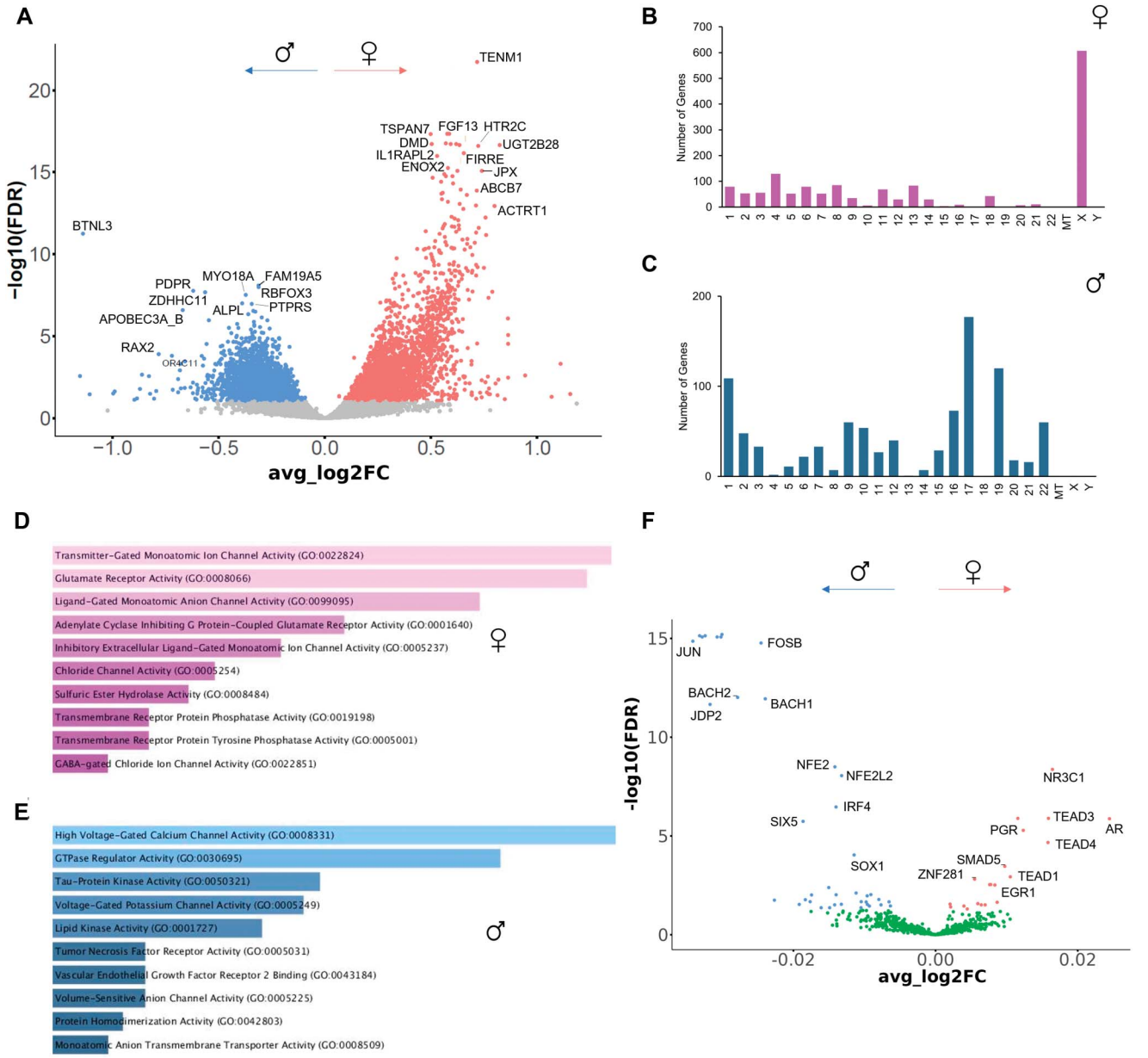

Figure 6. Sex differences in spatial ATAC-seq DARs in the neuronal cluster. (A) Volcano plot showing DARs in spatial ATAC-seq neuronal clusters in hDRG neurons in women vs men (N = 3 female, 5 male postmortem hDRGs), $P_{adj} < 0.01$ identified with ArchR. (B) Genome location of DARs in female neuronal ATAC-seq spanning the human chromosomes generated with ShinyGO. (C) Genomic position of the DAR gene set in men. (D) Overview of the molecular function gene ontology for DAR-associated genes in female neurons in hDRG. (E) Summary of the gene ontology related to molecular functions for DAR-associated genes in male neurons in hDRG. (F) Volcano plot showing transcription factor binding site enrichment in DARs in hDRG neurons in women vs men (N = 3, 5 male hDRGs), $P_{adj} < 0.1$ identified with ArchR. ATAC-seq, assays for transposase-accessible chromatin technology followed by sequencing; DAR, differentially accessible region; hDRG, human dorsal root ganglion.

3.8. Patterns of chromatin accessibility in human dorsal root ganglion are moderately positively correlated to the transcriptomic profile

In light of the sex dimorphic differences in chromatin accessibility between sexes in our bulk ATAC-seq results, we conducted a differential gene expression analysis on bulk nuclear RNA-seq (nucRNA-seq). RNA extractions and sequencing were performed in nuclei extracted from DRGs of 7 donors (N = 3 women, N = 4 men (same set of donors as in bulk ATAC-seq; details in Table S1, http://links.lww.com/PAIN/C195). We found 8 genes that were statistically different between sexes in the nuclear compartment ($P_{adj} < 0.05$, fold change >1.33, Dataset S5, http://links.lww.com/PAIN/C195). Women showed higher expression of chemokine genes such as *CCL3* and *CCL4*. As expected, we found the X-inactive specific transcript (*XIST*) to be differentially expressed compared with men. An interesting point to highlight is that *EGR1* and *EGR3* were trending to be highly expressed in women compared with men in our RNA-seq data (Fig. S4A, http://links.lww.com/PAIN/C196), which aligns well with transcription factor footprints in ATAC-seq datasets and in situ hybridization experiments. On the other hand, men showed higher gene expression of pseudogenes and novel transcripts.

We tested the correlation between the log2 fold change in DARs situated in promoter and within gene bodies,[28] including exon, and intron regions in ATAC-seq and the log2 fold change in nucRNA-seq for those genes in the matched hDRG samples. We found a weak positive correlation between the transcriptional and the chromatin

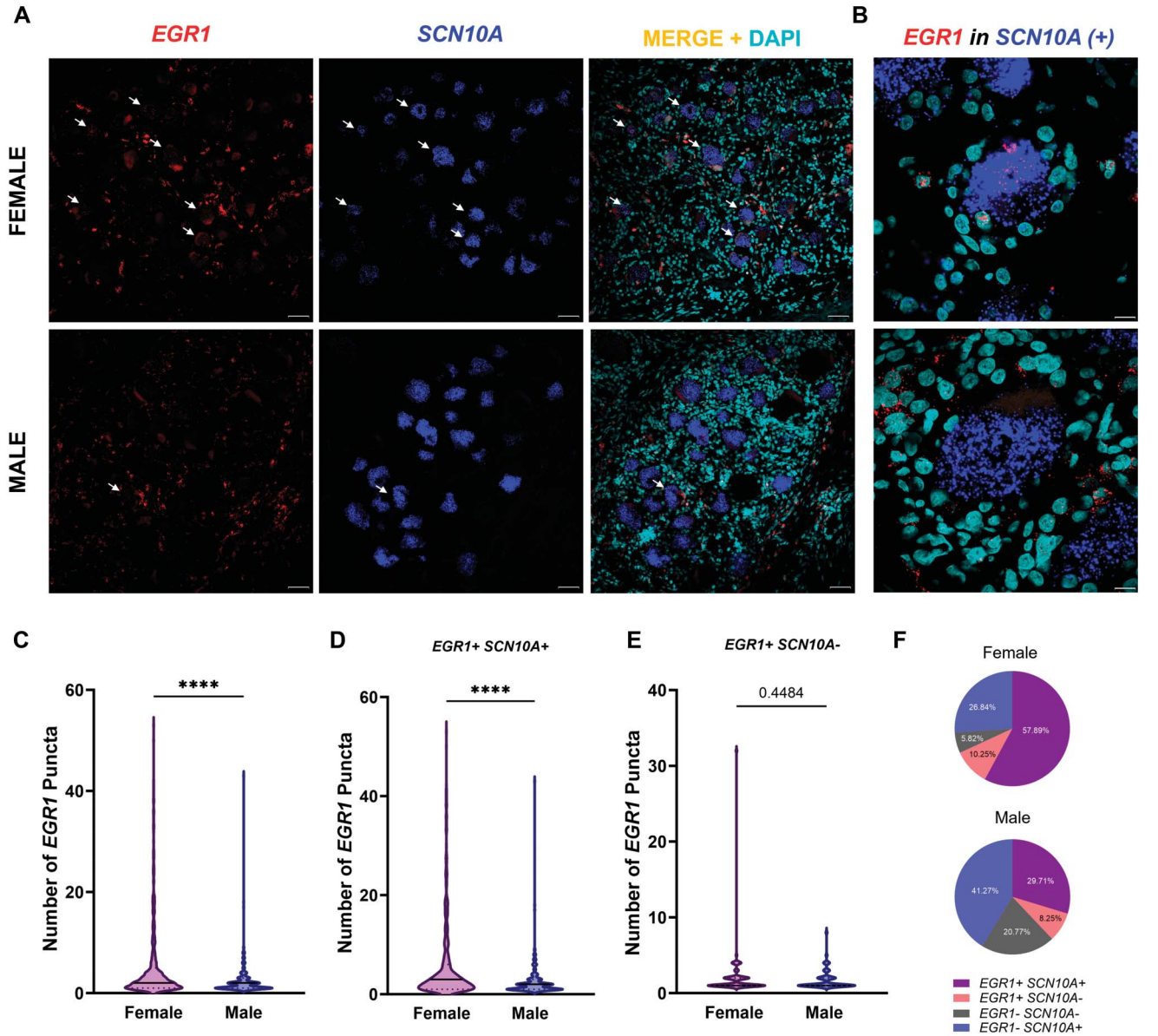

Figure 7. *EGR1* is expressed in more SCN10A positive neurons in women compared with men in hDRG. (A) Representative in situ hybridization images of *EGR1* (red) in *SCN10A*(+) neurons (blue) in female and male hDRG. *EGR1*(+) neurons are indicated with an arrow. (B) 100× magnification of neurons with *EGR1* mRNAs in female and male neurons. (C) Total number of *EGR1* mRNAs in neurons. (D and E) Number of *EGR1* mRNAs in *SCN10A*(+) and *SCN10A*(−) neurons, respectively. (F) Percentage of *EGR1*(+) positive cells in *SCN10A*(+) or *SCN10A*(−) cells across female and male donors in hDRG. A total of 722 neurons were analyzed to assess *EGR1* expression in female hDRG, and 727 in men (N = 5 female, N = 5 male DRG). Data are presented as violin plots with thick line indicating the median and the dotted lines indicating the quartiles. Section thickness—20 μm. Scale bar—50 μm for (A) and 10 μm for (B). ****$P < 0.0001$ as determined by *t* test in (C–E). hDRG, human dorsal root ganglion.

accessibility profiling (Fig. S4B, http://links.lww.com/PAIN/C196). This weak correlation could be explained by the repertoire of RNAs analyzed, which were limited to nuclear space and not to the whole cell. Evidence has shown that the nuclear compartment harbors abundant lncRNAs and small nucleolar RNAs in human brain tissue, consistent with the expressed genes in our nucRNA-seq data, while the cytoplasm contains RNAs associated with cellular functions such as metabolism, translation, and protein organization compared with the nuclear compartment.[91]

3.9. XIST *nuclear dispersion in female human dorsal root ganglion neurons*

Assays for transposase-accessible chromatin technology followed by sequencing datasets showed high accessibility for many X chromosome genes selectively in women, suggesting incomplete inactivation of the X chromosome at the foundational layer of the epigenome in human female DRG cells.[2] We explored the expression and localization of XIST RNA in hDRG because it controls X inactivation to achieve gene dosage compensation between sexes by coating, compacting, and sending 1 X chromosome to the periphery of the nuclei in female cells.[61,66] This compaction and localization in the nucleus ensures that 1 X chromosome in women remains in the heterochromatic or inactive state. Although *XIST* is generally considered an exclusive long noncoding RNA in women, *XIST* has been shown to be lowly expressed in male nerve tissue.[68] We performed in situ hybridization for *XIST* in female and male hDRG. In women, *XIST* was expressed in neuronal and nonneuronal cells

(**Fig. 8A**). Strikingly, we observed that the *XIST* signal was not confined to a single area inside the neuronal nuclei. Instead, the *XIST* signal was dispersed covering most of the nuclear compartment (**Fig. 8B**). This phenomenon was observed in *SCN10A* (+) and *SCN10A* (−) cells, where *XIST* spanned approximately 80% of the nuclear space. This observation was different in the cells surrounding the neurons, where the *XIST* signal was more confined, being restricted to around 20% of the nuclear space (**Fig. 8C**). As expected, compared with women, *XIST* was barely detected in male hDRG (Fig. S5, http://links.lww.com/PAIN/C196). As the dispersion of *XIST* RNA in the nucleus is associated with incomplete X inactivation,[77] these findings support the idea that hDRG neurons in women have incomplete X inactivation at the chromatin level, consistent with our ATAC-seq findings. The functions of *XIST* in hDRG in physiological and pathological conditions remain to be studied. Future experiments will be required to understand X inactivation mechanisms in hDRG neurons and how these impact gene expression levels in the female hDRG in physiological and pathological conditions. It is notable that animal models of pain have found the participation of *XIST* in inflammatory chronic pain.[40,73,76,86] Understanding this phenomenon in humans will lead to better insight into a potentially primed, accessible state for many genes ready to be activated by specific signals in the X chromosome in female hDRG.

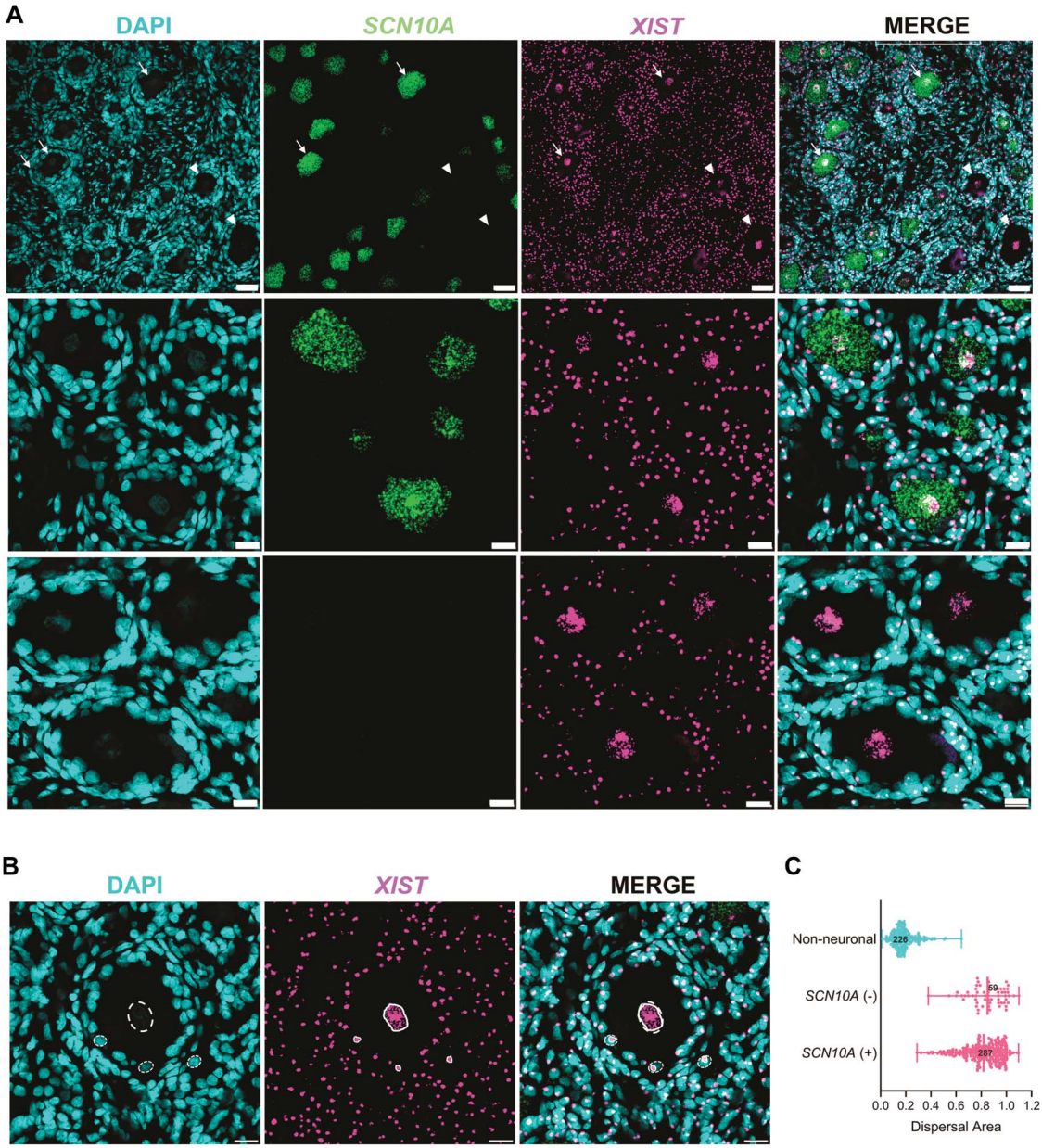

Figure 8. *XIST* is highly dispersed in the nuclear compartment of female neurons in hDRG. (A) Representative in situ hybridization images of *XIST* (magenta) in *SCN10A*(+) and *SCN10A*(−) neurons (green) in female hDRG (20× images [top], and 3× zoom magnification [bottom]). *XIST*(+) neurons, also positive for *SCN10A*, are indicated with an arrow. *XIST*(+) neurons, negative for *SCN10A*, are indicated with an arrowhead. (B) Representation of *XIST* dispersal analysis: an ROI was drawn around the nuclear compartment of neurons and nonneuronal cells (white). To delineate *XIST* area dispersion, we drew an ROI with the dots that were furthest apart from each other (white). (C) Representation of *XIST* dispersal area in *SCN10A*(+) and *SCN10A*(−) neurons and nonneuronal cells. A total of 346 neurons were analyzed to assess *XIST* expression and 226 nonneuronal cells in female hDRG (N = 3 female hDRG). Data are presented as scatter plots with lines indicating the mean and quartiles. Section thickness—10 μm. Scale bar—50 μm for (A) top and 20 μm for (A) bottom, and 20 μm for (B). hDRG, human dorsal root ganglion.

4. Discussion

Our work provides a comprehensive view of the chromatin accessibility profile in hDRG and focuses on sex differences in tissues recovered from organ donors without any history of chronic pain or neuropathy. We mapped the accessible DNA in hDRG using 2 different approaches, bulk and spatial ATAC-seq. The latter approach resolved hDRG chromatin accessible profiles in distinct cell types where we focused on neuronal signatures. First, our work shows a dimorphism at the chromatin level between sexes in hDRG. This dimorphism is largely influenced by the X chromosome in female hDRG suggesting a reduced X inactivation or a dormant transcriptional state that can readily become activated under certain circumstances. Second, our ATAC-seq data show a sex dimorphic signature in transcription factor bindings sites in accessible chromatin. EGR and SP motifs were more prominent in female hDRG, while AP-1 and IRF were more abundant in males. Finally, our work shows sex differences in neuronal chromatin using spatial ATAC-seq. In neurons, sex differences were partly driven by the X chromosome in women but using this approach we also uncovered differences in autosomal genes. GABA-A channels and glutamatergic genes were the molecular ontologies associated with accessible DNA in women, while voltage-gated Ca^{2+} and K^{+} channel genes as well as GTP-associated proteins were associated with male hDRG open chromatin.

Our bulk ATAC-seq findings point to a high chromatin accessibility in the X chromosome in women. Independently, spatial ATAC-seq confirmed this finding. It is known that 1 of the 2 X chromosomes in women is epigenetically silenced to compensate for the imbalance of X dosage between sexes.[61] X inactivation is triggered by the upregulation of *XIST* early in development. *XIST* coats 1 of the X chromosomes in *cis*[66,71] inducing X heterochromatization through repressive epigenetic signatures.[59] Interestingly, a small subgroup of genes escapes inactivation and has epigenetic marks of active transcription, allowing gene expression from the inactive X (Xi) chromosome.[2] Our findings are consistent with previous observations showing tissue-specific varying levels of X inactivation in human tissues.[82] Strikingly, *XIST* was found highly dispersed in the neuronal nuclei but not in the nuclei of surrounding cells in hDRG. *XIST* dispersion has been observed in human pluripotent cells,[17] where it has been hypothesized that *XIST* regulates autosomal genes in women. Our results are also consistent with a recent study showing greater variability in X inactivation in excitatory neurons in the human brain suggesting enhanced expression of genes from this chromosome in women in this population of neurons that share a glutamatergic biochemical phenotype with DRG neurons.[87] Importantly, a previous study linked X inactivation escape in blood cells to the development of chronic pain after a motor vehicle accident supporting the relevance of this line of investigation to pain.[90]

A fundamental challenge in pain research is identifying why women are more predisposed to pain. Studies in rodents have described that rapid transcriptional changes occur in DRG after injury suggesting a fast onset of transcriptional reprogramming.[11] A similar process could occur in humans and given the differences in the epigenetic landscape of the hDRG observed here, a testable hypothesis would be that this response could differ between men and women. We observed higher chromatin accessibility in women in genes coding for GABA-A receptor subunits, glutamatergic, and interferon-related genes, some of which are located on the X chromosome. This difference in interferon-related genes has been found in previous studies of the immune system.[23] Furthermore, previous findings from our group showed that interferon-related genes are more highly expressed in female hDRG from neuropathic pain patients undergoing thoracic vertebrectomy surgery.[64] Some of the female-biased genes were associated with DARs on autosomes, such as *GABRA5*. It has been shown that the α_5-$GABA_A$ receptor (encoded by the *Gabra5* gene in mice) is more highly expressed in the female rodent DRG where it plays an important role in pain signaling and is epigenetically regulated in a sex-specific fashion.[19,20] We also found higher accessibility in autosomal *BDNF-AS*, a *BDNF* suppressor. BDNF is released from primary afferents[37] binding to TrkB in spinal cord neurons regulating synaptic plasticity important for chronic pain.[14] Therefore, *BDNF-AS* could be an unappreciated suppressor of BDNF expression in women, a relevant finding because the role of BDNF signaling is more prominent in nociceptive signaling in male humans[15] and rodents.[43,53]

At the level of transcription factor footprints, EGR1/3 and SP showed higher abundance in female-accessible DNA in hDRG. In agreement with this, *EGR1* expression was higher in women. A recent study found that the expression of *Egr1* is driven by female sex hormones and acts as a chromatin modifier in a sex-specific fashion,[65] suggesting its pivotal role in controlling neuronal gene expression in women. Our data show that EGR1 binding sites are found in genes like *JAK1,* consistent with human thoracic vertebrectomy DRG data showing that interferon and JAK-STAT signaling are associated with neuropathic pain in women.[64] In addition, consistent with our findings, *SP4* has a higher expression in female tibial nerve compared with men.[63] SP4 regulates the transcription of genes that act as sensors of noxious stimuli[12] suggesting an important role of this protein to the transduction of nociceptive pain, while also contributing to persistent models of pain in mice.[72]

In men, we observed higher chromatin accessibility in transient receptor potential (TRP) channel-, *NTRK1*, and Ca^{2+}-related genes in hDRG, with some of them being specifically more accessible in neurons. TRP channel genes play important roles in encoding neuronal responses to noxious thermal stimuli. Cumulative evidence indicates that the function of TRP channel genes is modulated differentially between sexes, partly due to the influence of sex hormones.[10] However, the underlying molecular mechanisms are still to be uncovered, and our findings suggest a possible chromatin architecture explanation. In line with our results, *NTRK1* is more abundant in men in the human tibial nerve.[63] At the level of transcriptional programs, AP-1 transcription factors were predominant in male hDRG in both bulk and spatial ATAC-seq specifically in neurons. These data are in close agreement with increased JUN and FOS-activated transcriptional cascades in DRGs from male patients with neuropathic pain in a thoracic vertebrectomy cohort.[64] We found that the promoters of genes such as *OSMR* or *NLRP3* are predicted to be bound by these transcription factors. The abundance of binding sites for these genes in male open chromatin in the DRG correlates with the increased OSM signaling specifically upregulated in men in the thoracic vertebrectomy cohort.[55,64]

Collectively, our data demonstrate distinct baseline sex-specific chromatin accessibility patterns and transcriptional programs in hDRG. Differences observed in female hDRG, such as increased accessibility of GABAergic, glutamatergic, and interferon-related genes, could contribute to their heightened susceptibility to pain, a hypothesis that can be tested in the future. Conversely, higher accessibility of *TRP* and *NTRK1* genes in men might underlie distinct nociceptive pain mechanisms. These findings highlight fundamental sex differences in the epigenomic architecture of the human peripheral nervous system with implications for understanding sex differences in clinical pain disorders.

5. Limitations

This study has multiple limitations. First, we did not assess differences in chromatin accessibility between pain and nonpain hDRG samples. Our future studies will analyze whether the chromatin features in genes from our current work participate in chronic pain. Second, we did not perform multiomics from the same cell, making it difficult to test for a direct correlation between gene expression and chromatin accessibility. We tried to partially address this issue by correlating RNA and accessible chromatin from the same DRGs; however, the correlation was low, probably due to the small sample size. Another explanation for the low correlation is that accessible regions are not necessarily associated with actively transcribed genes, or they are associated with genes that are poised to become active under specific conditions.[74] It can also be the case where the transcription factor needed to activate gene transcription of accessible genes may be lacking in a particular cell state, but turned on in another, such as after injury. Our work here can be viewed as an important starting point for understanding the epigenome of the hDRG. Further research combining spatial and single-cell assessment of different histone marks, other DNA modifications, and interactions with transcription factors will be required to fully understand the epigenomic landscape of human nociceptors and to get a better interpretation of gene regulation in this complex tissue. Finally, our data provide evidence of X inactivation escape in hDRG neurons of women, but this idea should be tested with experimental manipulations, potentially in cultured hDRG neurons, to better understand its functional consequences and mechanisms.

Conflict of interest statement

The authors declare no financial conflicts of interest related to this work.

Acknowledgements

The authors acknowledge Yeunhee Kim, Manager of the Genome Center at the University of Texas at Dallas for technical support with library prep for sequencing. The authors acknowledge Jennifer Garbarino, Andrés Hernández-Oliveras, Abhira Ravirala, and Zawge Yohannes Daniel for technical support on this project. The authors thank Anna Cervantes, Geoffrey Funk, and Peter Horton at the Southwest Transplant Alliance. The authors are grateful to the organ donors and their families for their gifts. Data availability: Data in this study is available in the SPARC Portal at doi:10.26275/vi5j-qxw7. This study was supported by the National Institutes of Health grant U19NS130608 and R01NS111929 to T.J.P.

Author contributions: Ú.F.-E. and T.J.P. designed research project; Ú.F.-E. conducted ATAC-seq and RNA-seq experiments; Ú.F.-E., N.N.I., and J.C.M.S. performed computational analysis; Ú.F.-E. and K.N. performed in situ hybridization experiments; J.M. and K.M. supplied computational feedback; J.C.M.S. and M.S. provided insight to this study; Ú.F.-E. and T.J.P. wrote the manuscript.

Supplemental digital content

Supplemental digital content associated with this article can be found online at http://links.lww.com/PAIN/C195 and http://links.lww.com/PAIN/C196.

Supplemental video content

A video abstract associated with this article can be found on the PAIN Web site.

Article history:
Received 17 July 2024
Received in revised form 27 September 2024
Accepted 14 October 2024
Available online 23 January 2025

References

[1] Adey A, Morrison HG, Asan XunX, Xun X, Kitzman JO, Turner EH, Stackhouse B, MacKenzie AP, Caruccio NC, Zhang X, Shendure J. Rapid, low-input, low-bias construction of shotgun fragment libraries by high-density in vitro transposition. Genome Biol 2010; 11:R119.
[2] Balaton BP, Brown CJ. Escape artists of the X chromosome. Trends Genet 2016;32:348–59.
[3] Barter MJ, Cheung K, Falk J, Panagiotopoulos AC, Cosimini C, O'Brien S, Teja-Putri K, Neill G, Deehan DJ, Young DA. Dynamic chromatin accessibility landscape changes following interleukin-1 stimulation. Epigenetics 2021;16:106–19.
[4] Bartley EJ, Fillingim RB. Sex differences in pain: a brief review of clinical and experimental findings. Br J Anaesth 2013;111:52–8.
[5] Bentsen M, Goymann P, Schultheis H, Klee K, Petrova A, Wiegandt R, Fust A, Preussner J, Kuenne C, Braun T, Kim J, Looso M. ATAC-seq footprinting unravels kinetics of transcription factor binding during zygotic genome activation. Nat Commun 2020;11:4267.
[6] Berkley KJ. Sex differences in pain. Behav Brain Sci 1997;20:371–513; discussion 435–513.
[7] Bhuiyan SA, Xu M, Yang L, Semizoglou E, Bhatia P, Pantaleo KI, Tochitsky I, Jain A, Erdogan B, Blair S, Cat V, Mwirigi JM, Sankaranarayanan I, Tavares-Ferreira D, Green U, McIlvried LA, Copits BA, Bertels Z, Del Rosario JS, Widman AJ, Slivicki RA, Yi J, Sharif-Naeini R, Woolf CJ, Lennerz JK, Whited JL, Price TJ, Robert WGI, Renthal W. Harmonized cross-species cell atlases of trigeminal and dorsal root ganglia. Sci Adv 2024;10(25):eadj9173.
[8] Buenrostro JD, Giresi PG, Zaba LC, Chang HY, Greenleaf WJ. Transposition of native chromatin for fast and sensitive epigenomic profiling of open chromatin, DNA-binding proteins and nucleosome position. Nat Methods 2013;10:1213–8.
[9] Buenrostro JD, Wu B, Chang HY, Greenleaf WJ. ATAC-seq: a method for assaying chromatin accessibility genome-wide. Curr Protoc Mol Biol 2015;109:21.29.1–21.29.9.
[10] Cabanero D, Villalba-Riquelme E, Fernandez-Ballester G, Fernandez-Carvajal A, Ferrer-Montiel A. ThermoTRP channels in pain sexual dimorphism: new insights for drug intervention. Pharmacol Ther 2022; 240:108297.
[11] Chernov AV, Shubayev VI. Sexual dimorphism of early transcriptional reprogramming in dorsal root ganglia after peripheral nerve injury. Front Mol Neurosci 2021;14:779024.
[12] Chu C, Zavala K, Fahimi A, Lee J, Xue Q, Eilers H, Schumacher MA. Transcription factors Sp1 and Sp4 regulate TRPV1 gene expression in rat sensory neurons. Mol Pain 2011;7:44.
[13] Corces MR, Trevino AE, Hamilton EG, Greenside PG, Sinnott-Armstrong NA, Vesuna S, Satpathy AT, Rubin AJ, Montine KS, Wu B, Kathiria A, Cho SW, Mumbach MR, Carter AC, Kasowski M, Orloff LA, Risca VI, Kundaje A, Khavari PA, Montine TJ, Greenleaf WJ, Chang HY. An improved ATAC-seq protocol reduces background and enables interrogation of frozen tissues. Nat Methods 2017;14:959–62.
[14] Coull JA, Beggs S, Boudreau D, Boivin D, Tsuda M, Inoue K, Gravel C, Salter MW, De Koninck Y. BDNF from microglia causes the shift in neuronal anion gradient underlying neuropathic pain. Nature 2005;438: 1017–21.
[15] Dedek A, Xu J, Lorenzo LE, Godin AG, Kandegedara CM, Glavina G, Landrigan JA, Lombroso PJ, De Koninck Y, Tsai EC, Hildebrand ME. Sexual dimorphism in a neuronal mechanism of spinal hyperexcitability across rodent and human models of pathological pain. Brain 2022;145: 1124–38.
[16] Deng Y, Bartosovic M, Ma S, Zhang D, Kukanja P, Xiao Y, Su G, Liu Y, Qin X, Rosoklija GB, Dwork AJ, Mann JJ, Xu ML, Halene S, Craft JE, Leong KW, Boldrini M, Castelo-Branco G, Fan R. Spatial profiling of chromatin accessibility in mouse and human tissues. Nature 2022;609:375–83.

[17] Dror I, Chitiashvili T, Tan SYX, Cano CT, Sahakyan A, Markaki Y, Chronis C, Collier AJ, Deng W, Liang G, Sun Y, Afasizheva A, Miller J, Xiao W, Black DL, Ding F, Plath K. XIST directly regulates X-linked and autosomal genes in naive human pluripotent cells. Cell 2024;187:110–29.e31.
[18] Fillingim RB, King CD, Ribeiro-Dasilva MC, Rahim-Williams B, Riley JL III. Sex, gender, and pain: a review of recent clinical and experimental findings. J Pain 2009;10:447–85.
[19] Franco-Enzastiga U, De la Luz-Cuellar YE, Hernandez Reyes LE, Raya-Tafolla G, Torres-Lopez JE, Murbartian J, Granados-Soto V, Delgado-Lezama R. Extrasynaptic α5GABAA receptors and their role in nociception and pathological pain. In: Rajendram R, Preedy VR, Patel V, Martin CR, editors. The Neurobiology, Physiology, and Psychology of Pain. San Diego, CA: Academic Press, 2022. p. 129–37.
[20] Franco-Enzastiga U, Garcia G, Murbartian J, Gonzalez-Barrios R, Salinas-Abarca AB, Sanchez-Hernandez B, Tavares-Ferreira D, Herrera LA, Barragan-Iglesias P, Delgado-Lezama R, Price TJ, Granados-Soto V. Sex-dependent pronociceptive role of spinal α_5 -$GABA_A$ receptor and its epigenetic regulation in neuropathic rodents. J Neurochem 2021;156:897–916.
[21] Franco-Enzastiga U, Price T. Human dorsal root ganglion bulk ATAC-seq protocol. Berkley, CA: Protocolsio, 2024.
[22] Franco-Enzastiga U, Price T. Human dorsal root ganglion spatial ATAC-seq protocol. Berkley, CA: Protocolsio, 2024.
[23] Gal-Oz ST, Maier B, Yoshida H, Seddu K, Elbaz N, Czysz C, Zuk O, Stranger BE, Ner-Gaon H, Shay T. ImmGen report: sexual dimorphism in the immune system transcriptome. Nat Commun 2019;10:4295.
[24] Ghazisaeidi S, Muley MM, Salter MW. Neuropathic pain: mechanisms, sex differences, and potential therapies for a global problem. Annu Rev Pharmacol Toxicol 2023;63:565–83.
[25] Ghosh K, Pan HL. Epigenetic mechanisms of neural plasticity in chronic neuropathic pain. ACS Chem Neurosci 2022;13:432–41.
[26] Gong L, Gao F, Li J, Li J, Yu X, Ma X, Zheng W, Cui S, Liu K, Zhang M, Kunze W, Liu CY. Oxytocin-induced membrane hyperpolarization in pain-sensitive dorsal root ganglia neurons mediated by Ca(2+)/nNOS/NO/KATP pathway. Neuroscience 2015;289:417–28.
[27] Grandi FC, Modi H, Kampman L, Corces MR. Chromatin accessibility profiling by ATAC-seq. Nat Protoc 2022;17:1518–52.
[28] Granja JM, Corces MR, Pierce SE, Bagdatli ST, Choudhry H, Chang HY, Greenleaf WJ. ArchR is a scalable software package for integrative single-cell chromatin accessibility analysis. Nat Genet 2021;53:403–11.
[29] Greenspan JD, Craft RM, LeResche L, Arendt-Nielsen L, Berkley KJ, Fillingim RB, Gold MS, Holdcroft A, Lautenbacher S, Mayer EA, Mogil JS, Murphy AZ, Traub RJ, Consensus Working Group of the Sex Gender and Pain SIG of the IASP. Studying sex and gender differences in pain and analgesia: a consensus report. PAIN 2007;132(suppl 1):S26–45.
[30] Gregus AM, Levine IS, Eddinger KA, Yaksh TL, Buczynski MW. Sex differences in neuroimmune and glial mechanisms of pain. PAIN 2021;162:2186–200.
[31] Guekos A, Saxer J, Salinas Gallegos D, Schweinhardt P. Healthy women show more experimentally induced central sensitization compared with men. PAIN 2024;165:1413–24.
[32] Hauberg ME, Creus-Muncunill J, Bendl J, Kozlenkov A, Zeng B, Corwin C, Chowdhury S, Kranz H, Hurd YL, Wegner M, Borglum AD, Dracheva S, Ehrlich ME, Fullard JF, Roussos P. Common schizophrenia risk variants are enriched in open chromatin regions of human glutamatergic neurons. Nat Commun 2020;11:5581.
[33] Huang ZZ, Li D, Liu CC, Cui Y, Zhu HQ, Zhang WW, Li YY, Xin WJ. CX3CL1-mediated macrophage activation contributed to paclitaxel-induced DRG neuronal apoptosis and painful peripheral neuropathy. Brain Behav Immun 2014;40:155–65.
[34] Jung M, Dourado M, Maksymetz J, Jacobson A, Laufer BI, Baca M, Foreman O, Hackos DH, Riol-Blanco L, Kaminker JS. Cross-species transcriptomic atlas of dorsal root ganglia reveals species-specific programs for sensory function. Nat Commun 2023;14:366.
[35] Klemm SL, Shipony Z, Greenleaf WJ. Chromatin accessibility and the regulatory epigenome. Nat Rev Genet 2019;20:207–20.
[36] Kuleshov MV, Jones MR, Rouillard AD, Fernandez NF, Duan Q, Wang Z, Koplev S, Jenkins SL, Jagodnik KM, Lachmann A, McDermott MG, Monteiro CD, Gundersen GW, Ma'ayan A. Enrichr: a comprehensive gene set enrichment analysis web server 2016 update. Nucleic Acids Res 2016;44:W90–7.
[37] Latremoliere A, Woolf CJ. Central sensitization: a generator of pain hypersensitivity by central neural plasticity. J Pain 2009;10:895–926.
[38] Laumet G, Garriga J, Chen SR, Zhang Y, Li DP, Smith TM, Dong Y, Jelinek J, Cesaroni M, Issa JP, Pan HL. G9a is essential for epigenetic silencing of K(+) channel genes in acute-to-chronic pain transition. Nat Neurosci 2015;18:1746–55.
[39] Lautenbacher S, Rollman GB. Sex differences in responsiveness to painful and non-painful stimuli are dependent upon the stimulation method. PAIN 1993;53:255–64.
[40] Liao J, Zhang F, Qing W, Yu R, Hu Z. Mechanism of incisional pain: novel finding on long noncoding RNA XIST/miR-340-5p/RAB1A Axis. ASN Neuro 2021;13:17590914211049056.
[41] Lopes DM, Malek N, Edye M, Jager SB, McMurray S, McMahon SB, Denk F. Sex differences in peripheral not central immune responses to pain-inducing injury. Sci Rep 2017;7:16460.
[42] Manners MT, Ertel A, Tian Y, Ajit SK. Genome-wide redistribution of MeCP2 in dorsal root ganglia after peripheral nerve injury. Epigenetics Chromatin 2016;9:23.
[43] Mapplebeck JCS, Lorenzo LE, Lee KY, Gauthier C, Muley MM, De Koninck Y, Prescott SA, Salter MW. Chloride dysregulation through downregulation of KCC2 mediates neuropathic pain in both sexes. Cell Rep 2019;28:590–6.e4.
[44] Margueron R, Reinberg D. Chromatin structure and the inheritance of epigenetic information. Nat Rev Genet 2010;11:285–96.
[45] Marquez EJ, Chung CH, Marches R, Rossi RJ, Nehar-Belaid D, Eroglu A, Mellert DJ, Kuchel GA, Banchereau J, Ucar D. Sexual-dimorphism in human immune system aging. Nat Commun 2020;11:751.
[46] Matsushita Y, Araki K, Omotuyi O, Mukae T, Ueda H. HDAC inhibitors restore C-fibre sensitivity in experimental neuropathic pain model. Br J Pharmacol 2013;170:991–8.
[47] Mecklenburg J, Zou Y, Wangzhou A, Garcia D, Lai Z, Tumanov AV, Dussor G, Price TJ, Akopian AN. Transcriptomic sex differences in sensory neuronal populations of mice. Sci Rep 2020;10:15278.
[48] Mich JK, Graybuck LT, Hess EE, Mahoney JT, Kojima Y, Ding Y, Somasundaram S, Miller JA, Kalmbach BE, Radaelli C, Gore BB, Weed N, Omstead V, Bishaw Y, Shapovalova NV, Martinez RA, Fong O, Yao S, Mortrud M, Chong P, Loftus L, Bertagnolli D, Goldy J, Casper T, Dee N, Opitz-Araya X, Cetin A, Smith KA, Gwinn RP, Cobbs C, Ko AL, Ojemann JG, Keene CD, Silbergeld DL, Sunkin SM, Gradinaru V, Horwitz GD, Zeng H, Tasic B, Lein ES, Ting JT, Levi BP. Functional enhancer elements drive subclass-selective expression from mouse to primate neocortex. Cel Rep 2021;34:108754.
[49] Mine-Hattab J, Chiolo I. Complex chromatin motions for DNA repair. Front Genet 2020;11:800.
[50] Mogil JS. Perspective: equality need not be painful. Nature 2016;535:S7.
[51] Mogil JS. Qualitative sex differences in pain processing: emerging evidence of a biased literature. Nat Rev Neurosci 2020;21:353–65.
[52] Mogil JS, Bailey AL. Sex and gender differences in pain and analgesia. Prog Brain Res 2010;186:141–57.
[53] Moy JK, Szabo-Pardi T, Tillu DV, Megat S, Pradhan G, Kume M, Asiedu MN, Burton MD, Dussor G, Price TJ. Temporal and sex differences in the role of BDNF/TrkB signaling in hyperalgesic priming in mice and rats. Neurobiol Pain 2019;5:100024.
[54] Nguyen MQ, von Buchholtz LJ, Reker AN, Ryba NJ, Davidson S. Single-nucleus transcriptomic analysis of human dorsal root ganglion neurons. Elife 2021;10:e71752.
[55] North RY, Li Y, Ray P, Rhines LD, Tatsui CE, Rao G, Johansson CA, Zhang H, Kim YH, Zhang B, Dussor G, Kim TH, Price TJ, Dougherty PM. Electrophysiological and transcriptomic correlates of neuropathic pain in human dorsal root ganglion neurons. Brain 2019;142:1215–26.
[56] Obeidat AM, Wood MJ, Adamczyk NS, Ishihara S, Li J, Wang L, Ren D, Bennett DA, Miller RJ, Malfait AM, Miller RE. Piezo2 expressing nociceptors mediate mechanical sensitization in experimental osteoarthritis. Nat Commun 2023;14:2479.
[57] Parisien M, Khoury S, Chabot-Dore AJ, Sotocinal SG, Slade GD, Smith SB, Fillingim RB, Ohrbach R, Greenspan JD, Maixner W, Mogil JS, Belfer I, Diatchenko L. Effect of human genetic variability on gene expression in dorsal root ganglia and association with pain phenotypes. Cel Rep 2017;19:1940–52.
[58] Patil M, Belugin S, Mecklenburg J, Wangzhou A, Paige C, Barba-Escobedo PA, Boyd JT, Goffin V, Grattan D, Boehm U, Dussor G, Price TJ, Akopian AN. Prolactin regulates pain responses via a female-selective nociceptor-specific mechanism. iScience 2019;20:449–65.
[59] Patrat C, Ouimette JF, Rougeulle C. X chromosome inactivation in human development. Development 2020;147:dev183095.
[60] Pieretti S, Di Giannuario A, Di Giovannandrea R, Marzoli F, Piccaro G, Minosi P, Aloisi AM. Gender differences in pain and its relief. Ann Ist Super Sanita 2016;52:184–9.
[61] Popova BC, Tada T, Takagi N, Brockdorff N, Nesterova TB. Attenuated spread of X-inactivation in an X;autosome translocation. Proc Natl Acad Sci U S A 2006;103:7706–11.
[62] Qiu F, Qiu CY, Cai H, Liu TT, Qu ZW, Yang Z, Li JD, Zhou QY, Hu WP. Oxytocin inhibits the activity of acid-sensing ion channels through the

vasopressin, V1A receptor in primary sensory neurons. Br J Pharmacol 2014;171:3065–76.
[63] Ray PR, Khan J, Wangzhou A, Tavares-Ferreira D, Akopian AN, Dussor G, Price TJ. Transcriptome analysis of the human tibial nerve identifies sexually dimorphic expression of genes involved in pain, inflammation, and neuro-immunity. Front Mol Neurosci 2019;12:37.
[64] Ray PR, Shiers S, Caruso JP, Tavares-Ferreira D, Sankaranarayanan I, Uhelski ML, Li Y, North RY, Tatsui C, Dussor G, Burton MD, Dougherty PM, Price TJ. RNA profiling of human dorsal root ganglia reveals sex differences in mechanisms promoting neuropathic pain. Brain 2023;146:749–66.
[65] Rocks D, Purisic E, Gallo EF, Greally JM, Suzuki M, Kundakovic M. Egr1 is a sex-specific regulator of neuronal chromatin, synaptic plasticity, and behaviour. bioRxiv 2023:2023.12.20.572697. doi: 10.1101/2023.12.20.572697
[66] Rodermund L, Coker H, Oldenkamp R, Wei G, Bowness J, Rajkumar B, Nesterova T, Susano Pinto DM, Schermelleh L, Brockdorff N. Time-resolved structured illumination microscopy reveals key principles of XIST RNA spreading. Science 2021;372:eabe7500.
[67] Rosen S, Ham B, Mogil JS. Sex differences in neuroimmunity and pain. J Neurosci Res 2017;95:500–8.
[68] Sadagopan A, Nasim IT, Li J, Achom M, Zhang CZ, Viswanathan SR. Somatic XIST activation and features of X chromosome inactivation in male human cancers. Cell Syst 2022;13:932–44.e5.
[69] San Roman AK, Skaletsky H, Godfrey AK, Bokil NV, Teitz L, Singh I, Blanton LV, Bellott DW, Pyntikova T, Lange J, Koutseva N, Hughes JF, Brown L, Phou S, Buscetta A, Kruszka P, Banks N, Dutra A, Pak E, Lasutschinkow PC, Keen C, Davis SM, Lin AE, Tartaglia NR, Samango-Sprouse C, Muenke M, Page DC. The human Y and inactive X chromosomes similarly modulate autosomal gene expression. Cell Genom 2024;4(1):100462.
[70] Schang AL, Saberan-Djoneidi D, Mezger V. The impact of epigenomic next-generation sequencing approaches on our understanding of neuropsychiatric disorders. Clin Genet 2018;93:467–80.
[71] Schwammle T, Schulz EG. Regulatory principles and mechanisms governing the onset of random X-chromosome inactivation. Curr Opin Genet Dev 2023;81:102063.
[72] Sheehan K, Lee J, Chong J, Zavala K, Sharma M, Philipsen S, Maruyama T, Xu Z, Guan Z, Eilers H, Kawamata T, Schumacher M. Transcription factor Sp4 is required for hyperalgesic state persistence. PLoS One 2019;14:e0211349.
[73] Shenoda BB, Ramanathan S, Gupta R, Tian Y, Jean-Toussaint R, Alexander GM, Addya S, Somarowthu S, Sacan A, Ajit SK. XIST attenuates acute inflammatory response by female cells. Cell Mol Life Sci 2021;78:299–316.
[74] Starks RR, Biswas A, Jain A, Tuteja G. Combined analysis of dissimilar promoter accessibility and gene expression profiles identifies tissue-specific genes and actively repressed networks. Epigenetics Chromatin 2019;12:16.
[75] Stephens KE, Zhou W, Renfro Z, Ji Z, Ji H, Guan Y, Taverna SD. Global gene expression and chromatin accessibility of the peripheral nervous system in animal models of persistent pain. J Neuroinflammation 2021;18:185.
[76] Sun W, Ma M, Yu H, Yu H. Inhibition of lncRNA X inactivate-specific transcript ameliorates inflammatory pain by suppressing satellite glial cell activation and inflammation by acting as a sponge of miR-146a to inhibit Na(v) 1.7. J Cel Biochem 2018;119:9888–98.
[77] Sunwoo H, Colognori D, Froberg JE, Jeon Y, Lee JT. Repeat E anchors XIST RNA to the inactive X chromosomal compartment through CDKN1A-interacting protein (CIZ1). Proc Natl Acad Sci U S A 2017;114:10654–9.
[78] Tavares-Ferreira D, Ray PR, Sankaranarayanan I, Mejia GL, Wangzhou A, Shiers S, Uttarkar R, Megat S, Barragan-Iglesias P, Dussor G, Akopian AN, Price TJ. Sex differences in nociceptor translatomes contribute to divergent prostaglandin signaling in male and female mice. Biol Psychiatry 2022;91:129–40.
[79] Tavares-Ferreira D, Shiers S, Ray PR, Wangzhou A, Jeevakumar V, Sankaranarayanan I, Cervantes AM, Reese JC, Chamessian A, Copits BA, Dougherty PM, Gereau RWt, Burton MD, Dussor G, Price TJ. Spatial transcriptomics of dorsal root ganglia identifies molecular signatures of human nociceptors. Sci Transl Med 2022;14:eabj8186.
[80] Thibodeau A, Uyar A, Khetan S, Stitzel ML, Ucar D. A neural network based model effectively predicts enhancers from clinical ATAC-seq samples. Sci Rep 2018;8:16048.
[81] Tsang A, Von Korff M, Lee S, Alonso J, Karam E, Angermeyer MC, Borges GL, Bromet EJ, Demytteneare K, de Girolamo G, de Graaf R, Gureje O, Lepine JP, Haro JM, Levinson D, Oakley Browne MA, Posada-Villa J, Seedat S, Watanabe M. Common chronic pain conditions in developed and developing countries: gender and age differences and comorbidity with depression-anxiety disorders. J Pain 2008;9:883–91.
[82] Tukiainen T, Villani AC, Yen A, Rivas MA, Marshall JL, Satija R, Aguirre M, Gauthier L, Fleharty M, Kirby A, Cummings BB, Castel SE, Karczewski KJ, Aguet F, Byrnes A, GTEx Consortium; Laboratory, Data Analysis & Coordinating Center (LDACC)—Analysis Working Group; Statistical Methods groups—Analysis Working Group; Enhancing GTEx (eGTEx) groups; NIH Common Fund; NIH/NCI; NIH/NHGRI; NIH/NIMH; NIH/NIDA; Biospecimen Collection Source Site—NDRI; Biospecimen Collection Source Site—RPCI; Biospecimen Core Resource—VARI; Brain Bank Repository—University of Miami Brain Endowment Bank; Leidos Biomedical—Project Management; ELSI Study; Genome Browser Data Integration &Visualization—EBI; Genome Browser Data Integration &Visualization—UCSC Genomics Institute, University of California Santa Cruz, Lappalainen T, Regev A, Ardlie KG, Hacohen N, MacArthur DG. Landscape of X chromosome inactivation across human tissues. Nature 2017;550:244–8.
[83] Uchida H, Ma L, Ueda H. Epigenetic gene silencing underlies C-fiber dysfunctions in neuropathic pain. J Neurosci 2010;30:4806–14.
[84] Uchida H, Matsushita Y, Ueda H. Epigenetic regulation of BDNF expression in the primary sensory neurons after peripheral nerve injury: implications in the development of neuropathic pain. Neuroscience 2013;240:147–54.
[85] Valtcheva MV, Copits BA, Davidson S, Sheahan TD, Pullen MY, McCall JG, Dikranian K, Gereau RW IV. Surgical extraction of human dorsal root ganglia from organ donors and preparation of primary sensory neuron cultures. Nat Protoc 2016;11:1877–88.
[86] Wei M, Li L, Zhang Y, Zhang ZJ, Liu HL, Bao HG. LncRNA X inactive specific transcript contributes to neuropathic pain development by sponging miR-154-5p via inducing toll-like receptor 5 in CCI rat models. J Cel Biochem 2019;120:1271–81.
[87] Wen X, Luo Z, Zhao W, Calandrelli R, Nguyen TC, Wan X, Charles Richard JL, Zhong S. Single-cell multiplex chromatin and RNA interactions in ageing human brain. Nature 2024;628:648–56.
[88] Yan F, Powell DR, Curtis DJ, Wong NC. From reads to insight: a hitchhiker's guide to ATAC-seq data analysis. Genome Biol 2020;21:22.
[89] Yang L, Xu M, Bhuiyan SA, Li J, Zhao J, Cohrs RJ, Susterich JT, Signorelli S, Green U, Stone JR, Levy D, Lennerz JK, Renthal W. Human and mouse trigeminal ganglia cell atlas implicates multiple cell types in migraine. Neuron 2022;110:1806–21.e8.
[90] Yu S, Chen C, Pan Y, Kurz MC, Datner E, Hendry PL, Velilla MA, Lewandowski C, Pearson C, Domeier R, McLean SA, Linnstaedt SD. Genes known to escape X chromosome inactivation predict co-morbid chronic musculoskeletal pain and posttraumatic stress symptom development in women following trauma exposure. Am J Med Genet B Neuropsychiatr Genet 2019;180:415–27.
[91] Zaghlool A, Niazi A, Bjorklund AK, Westholm JO, Ameur A, Feuk L. Characterization of the nuclear and cytosolic transcriptomes in human brain tissue reveals new insights into the subcellular distribution of RNA transcripts. Sci Rep 2021;11:4076.
[92] Zhang H, Song L, Wang X, Cheng H, Wang C, Meyer CA, Liu T, Tang M, Aluru S, Yue F, Liu XS, Li H. Fast alignment and preprocessing of chromatin profiles with Chromap. Nat Commun 2021;12:6566.
[93] Zurek NA, Ehsanian R, Goins AE, Adams IM, Petersen T, Goyal S, Shilling M, Westlund KN, Alles SRA. Electrophysiological analyses of human dorsal root ganglia and human induced pluripotent stem cell-derived sensory neurons from male and female donors. J Pain 2024;25:104451.